STUDY OF ELECTROMAGNETIC FIELD MEASUREMENT METHODOLOGY OF PULSED ROTATING HIGH-POWER SIGNALS

by

PANTELAKI KALLIOPI

Electronic Engineer, Technological Educational Institute of Crete, 1997

A THESIS

submitted in partial fulfillment of the requirements for the degree

MASTER OF SCIENCE

DEPARTMENT OF INFORMATICS ENGINEERING

SCHOOL OF APPLIED TECHNOLOGY

TECHNOLOGICAL EDUCATIONAL INSTITUTE OF CRETE

2016

Approved by:

Major Professor
Dr. STRATAKIS DIMITRIOS

Abstract

The rapid growth of wireless communication technology has caused the increase of several types of wireless transmitter infrastructures. Several concerns have grown regarding the effects of electromagnetic fields exposure on human health. One special case of electromagnetic fields is that of pulsed rotating signals. Such emissions can be from aviation approach Radars, which often are in places close to populated areas. Due to the above facts, International Organizations and National legislation have adopted basic restrictions and reference levels for the maximum human exposure to electromagnetic fields.

The aim of this master thesis is to study the methodology that has to be applied for measuring electromagnetic fields from RADARs. Initially, a detailed study about the methodology of Radar measurements was made. Then, real measurements were carried out for testing purposes, with the use of the existing equipment of the "Non-Ionizing Radiation Laboratory of Technological Educational Institute (TEI) of Crete" (spectrum analyzer –SA- and appropriate antennas). The estimation of the electromagnetic burden of the Surveillance Radar (PSR) of Nikos Kazantzakis airport of Heraklion, Crete was examined. Optimal settings for the measurement equipment were investigated, selected, and validated. A method for the estimation of the overall uncertainty of the measurement for this type of emitted signals was also studied. Furthermore, a comparison of the measurement results with the legislated maximum limits of exposure was made. For this purpose, two dedicated software programs were developed in MATLAB, one for the remote control of the used instrumentation and the collection of the measurement data and the other for the processing of them. Finally, a method of measuring Radar with the channel power function of SA was studied and real measurements were carried out.

Measurements for the estimation of the electromagnetic burden of the Surveillance Radar (PSR) of Nikos Kazantzakis airport of Heraklion, Crete were performed for testing purposes.

Table of Contents

List of Figures

List of Tables

Acknowledgements

I would like to thank the faculty and administrative staff of the Department of Informatics Engineering of Technological Educational Institute of Heraklion, for their assistance during the postgraduate program “Informatics and Multimedia”. I would specifically like to thank my thesis supervisor, Dr. Dimitrios Stratakis for his valuable guidance and advice and the thesis committee members Dr. Evangelos Pallis and Dr. Georgios Mastorakis for their valuable input and assistance.

Dedication

This thesis work is dedicated to my husband, Fotis, who has been a constant source of support and encouragement during the challenges of this postgraduate program. This work is also dedicated to my children Georgia and Mariza. I am truly thankful for having you in my life. Last but not least I dedicate this work to my parents who are not in life anymore.

Thank you

Preface

The great development of wireless communication technology has caused much concern about the possible adverse effects of electromagnetic field exposure on human health. A special type of such emissions is the rotating pulsed signals, such as civil aviation approach Radars, often situated close to residential areas.

In this work, a detailed study was made for the methodology that has to be applied for measuring electromagnetic fields from RADARs. Then, real measurements were carried out with the use of the existing equipment of the "Non-Ionizing Radiation Laboratory of TEI of Crete" (spectrum analyzer and appropriate antennas). Finally, a comparison of the measurement results with the legislated maximum limits of exposure was made. For this purpose, two dedicated software programs were made in MATLAB, one for the remote control of the used instrumentation and the collection of the measurement data and the other for the processing of them.

In Chapter one, nowadays known biological Effects of Non- Ionizing Radiation to the human health are presented. In chapter two, the international and national standards are mentioned. In chapter three, the basic principles of Radar operation are described. In chapter four, the methods of pulsed Radar measurements and the appropriate instrumentation settings are examined. In chapter five, a method for the estimation of the measurement uncertainty is analyzed. In chapter six, a detailed description of Heraklion PSR Radar measurement is described. In chapter seven, the dedicated software application for PSR Radar measurements is presented. In chapter eight, a proposed method for Radar measurements with Channel Power function of SA is presented. Finally, in chapter nine the conclusions of this thesis along with thoughts for future work in the specific scientific area are outlined.

Chapter 1 –Biological Effects of Non- Ionizing Radiation

1.1 Electromagnetic Spectrum

The electromagnetic spectrum is the distribution of electromagnetic radiation according to energy. Radiation is energy that travels in the form of the electromagnetic waves (Figure 1.2) and spreads out as it goes [1]. The area where these waves are found is called electromagnetic field. The electromagnetic waves propagate with the speed of light. The range of the electromagnetic spectrum extends from very low frequencies (almost zero Hz) to very high (10^{24} Hz), as the figure 1.1 shows. It is divided at certain bands of frequency. These are: Radio waves (0-300GHz) and the part from 300MHz – 300GHz called Microwave, Infrared (300MHz – 400THz), Light (400THz- 800RHZ), Ultraviolet (800THz-$3*10^{17}$Hz), X-rays ($3*10^{17}$Hz - $5*10^{19}$Hz), Gamma rays ($5*10^{19}$Hz - $3*10^{22}$ Hz). The X-rays and Gamma rays are ionizing radiation. This type of radiation is radiation with enough energy so that during an interaction with an atom, it can remove tightly bound electrons from the orbit of an atom, causing the atom to become charged or ionized [2]. Therefore, it can break up the chemical bonds which appear in the molecules. On the other hand, the rest type of radiations are non – ionizing radiations. This means that, they cannot ionize the atom but they can cause some biological effects on the cells, plants, animals and people. The biological effects observed depend on many parameters of radiation (power, wavelength/frequency, near field - far field, pulsed fields, modulation, etc.) and have been tested for potential health effects [3]. In this work we studied measurement methods for the electromagnetic fields that an air traffic primary Radar emits. These kind of Radars work at the range of microwave band and have pulsed radiation.

Figure 1.1 Electromagnetic Spectrum

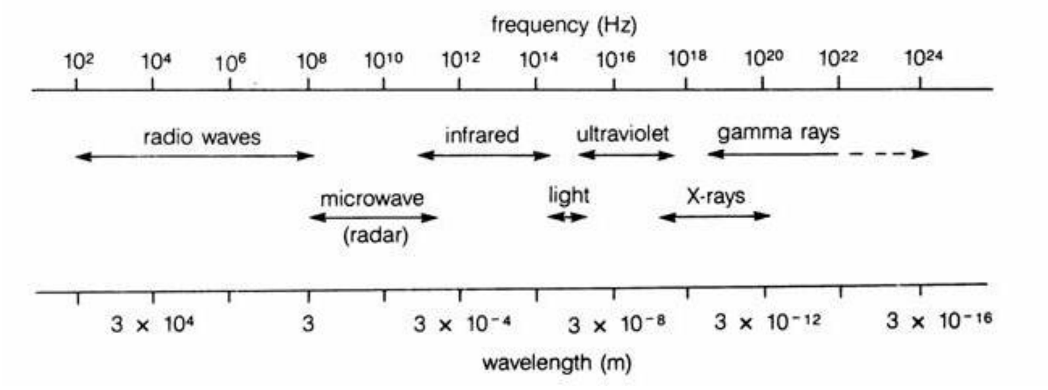

Figure 1.2 Electromagnetic Wave

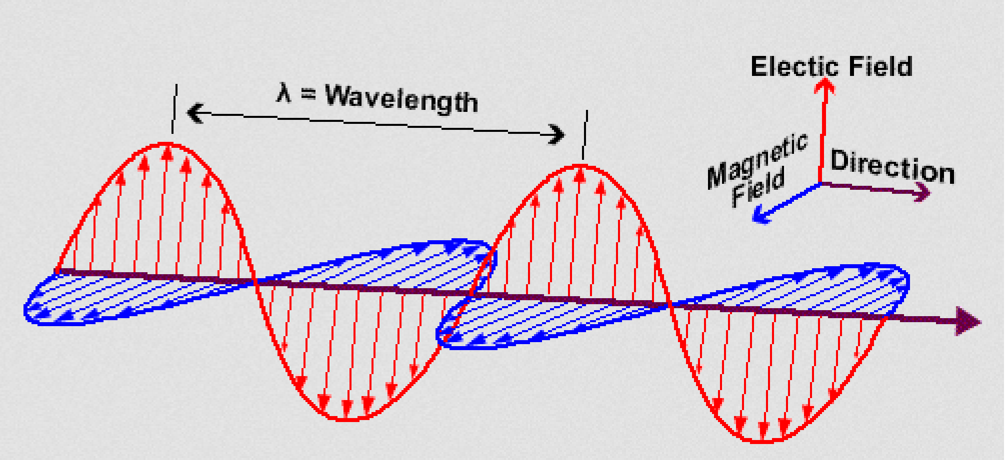

1.2 Biological Effects and Radiofrequencies

Since the 18th century scientists have noticed the effect of electromagnetic fields (EMFs) on humans, animals and plants. They have also observed that electromagnetic fields have different effects at different frequency ranges. Among them, the radiofrequency (RF) spectrum, particularly the range of microwave frequency, is an important part [4].

The biological effects of human exposure body and cells to the frequency range from 1MHz to 10GHz mainly depend on the frequency and intensity of electromagnetic fields. In this frequency range, the radiation is absorbed and penetrates to the body. The depth of penetration of the radiation depends on the frequency and is greater for lower frequencies. The energy of these electromagnetic fields is absorbed and causes the movement of the molecules. The collisions among rapidly moving molecules result in an increase of temperature. Two areas of the body, the eyes and testes, are particularly susceptible to RF heating as they are characterized by poor blood movement and therefore insufficient heat dissipation.

The quantity of energy deposition in the body is measured as Specific Absorption Rate (SAR). The unit of SAR is W/Kg. In the frequency area from 1MHz to 10GHz the SAR value should not exceed 4W/Kg so as negative adverse health effects on humans will not be raised up according to the nowadays scientific knowledge. Another quantity used in this frequency range is the Specific Absorption or SA, measured in Joule/kg and expresses the energy deposited in the tissues per unit mass [5]. The increased temperatures in the human body caused by the effects of electromagnetic radiation can have negative impacts. The increase in tissue temperature over 1°C for a long time can have a negative impact, regardless of its origin. It can even lead to reduced mental and physical condition, as studies have shown on workers in a hot environment. The increased temperatures may also have implications during embryonic development, as they can affect male fertility, or cause eye cataracts.

Intensity levels of the RF fields that are usually present in everyday environments are much weaker than those required to cause sufficient localized heating, or an increase in body temperature [5] [6].

On the other hand, apart from the noted thermal effects, today several studies on the existence of non-thermal effects of radio waves in biological tissues are conducted. Some studies have shown that, under certain conditions, the radio waves can cause non-thermal biological effects on cells or animals, without, however, being directly related to the existence of defects in the human body. Exposure to very low RF levels can alter calcium ion mobility, which is responsible for transmitting information in tissue cells. Such studies have been done mainly in Eastern Europe and Russia, the results of which are taken into consideration with national safety limits which have been established. In some of these studies, the results are displayed contradictory, while others could not be repeated. So, there is need for further studies on the non-thermal effects and their correlation with adverse biological effects and potential effects on health [5] [7]. The research continues worldwide in collaboration with the World Health Organization (WHO).

The electromagnetic radiation for frequencies greater than 10 GHz is absorbed by the surface of the skin and, as a result, very little penetrates the underlying tissues. The basic physical quantity of exposure to fields of these frequencies is the intensity of radiation measured as power density in W/m^2. Negative effects on human health, such as eye cataracts and skin burns, appear for power densities greater than 1000W/m^2. Such values are not found in everyday life.

1.3 Radiofrequencies and Cancer

A significant part of the population has questions about possible health effects from exposure to low intensity radio wave energy, corresponding to that present in the daily living environment. In the literature there are studies that suggest that it may cause various biological effects. Among them is the change of mobility of calcium ions, the rate of cell proliferation and activity of enzymes and their interaction with the DNA of the cells. These studies are equivocal and scientists have no conclusive results. However, there is public concern particularly about connecting radio frequency with cancer.

The results of recent studies on animal carcinogenicity are rather ambiguous and indicate that such effects on rodents are not likely at SAR levels up to 4W/kg. Studies relative to genotoxicity generally indicate a lack of effect [5] [8]. Today, the most widely accepted scientific view, is that exposure to low intensity radio frequency electromagnetic fields cannot cause or promote cancer.

1.3.1 Mobile phones and epidemiological studies

In autumn 2000 an international epidemiological research with the participation of 13 countries (called INTERPHONE study) was started in order to investigate the possible correlation between the regular and long - term use of mobile phones and the occurrence of brain cancer. The results from the UK, Sweden and Denmark were unable to relate the regular use of a mobile telephone with increased risk of brain cancer. In contrast, the

German survey showed an increased risk of glioma, a malignant type of brain cancer, among long-term mobile phone users (30 minutes per day over a 10-year period) [9].

On 31 May 2011, the WHO/International Agency for Research on Cancer (IARC) classified radiofrequency electromagnetic fields as possibly carcinogenic to humans, due to an increased risk of glioma [10].

Extensive epidemiological investigations have studied the occurrence of acoustic neuroma and its correlation with the use of mobile phones. The acoustic neuroma is a benign tumor of the auditory nerve. It may affect hearing. According to the results of several recent epidemiological investigations, there is no substantial risk of acoustic neuroma in the first decade of mobile phone use, but there is an increased risk after a ten years term of mobile phone use. In addition, there are no data on the possible carcinogenic effects of exposure to radiation of mobile phones in childhood and adolescence [5] [11].

1.4 Applications of Microwaves in Medicine

For many years we have used microwave technology in medicine for therapeutic purposes. Nowadays, new surveys are continuously made for new applications of microwaves in different treatments. The equipment used for medical diathermy in physiotherapy operates at 2450MHz. Moreover, several diseases have been effectively treated by microwaves, such as gastric, duodenal ulcer, cardiovascular diseases, respiratory diseases, tuberculosis, skin diseases etc [4].

The microwave thermotherapy has been used in medicine for the treatment of cancer and some other diseases since the early eighties. Another method used to treat cancer is hyperthermia. This method is based on the destruction of malignant cells by artificially elevated temperature in a temperature range between 41 and 45ºC fails self-protective mechanism of malignant cells. Hyperthermia is not limited by the number of radiation dose.

Also, many studies have been done on the use of microwave medical applications based on so-called non-thermal effects and the results are quite significant. Such investigations have been made to reduce the feeling of pain (analogically to analgesics), to increase reaction capabilities of a human being, to examine teaching capabilities, etc [12].

1.5 Biological Effects and Radar Systems

1.5.1 General Remarks

Radar systems detect the presence, direction, speed and distance of objects. They work by emitting high frequency electromagnetic waves. The radar is used in navigation, aviation, from the military and for weather forecasting.

People who live or usually work around radars have expressed concerns about the negative impact of these systems on health. Many questions have been raised whether the emission of radars is linked to cancer risk, reproductive malfunction, cataracts and changes in behavior or development of children.

Radars usually operate in the frequency range 300MHz-15GHz, namely in the RF band. Therefore, the biological effects that may be caused by the operation of the radars are the same as biological effects of radio frequencies in general.

It is important to distinguish if indeed there are risks from the operation of radars and to present the existing international standards and protective measures used today.

1.5.2 Human exposure

The mean power emitted by a radar system varies from a few mW (vehicle traffic control radar) to several kW. There are some factors that affect human exposure to the radiation of a radar:

- The radar emitting pulsed radiation, transmits an average power which is a lot lower than the corresponding peak (peak power).
- Radars are directional systems. The energy of RF radiation appears in beams that are very narrow. The radiation power density decreases drastically as we move away from the beam axis.
- Many radars have antennas whose beam continuously rotates or moves in the vertical plane.
- The areas where there may be a risk of radiation exposure are not accessible by unauthorized personnel [13].

1.5.3 Pulsed RF Fields

There have been various studies on the biological effects of pulsed radiation. Appropriate frequency pulse radiation and energy per pulse can cause the so-called microwave hearing effect. This auditory stimulus has been described in various ways by those who understand the characteristics according to the configuration of the radiation. So, the sound can be heard as a buzzing, clicking, hissing or popping sound. The phenomenon is appeared between the frequencies 200MHz and 6.5GHz. This phenomenon has been attributed to thermoelastic oscillation of the brain. It causes stress, but it is not known if it has other long-term effects on human health [13].

Also, the pulsed radiation can affect tissues of the eye in animals. In addition, the mice exposed to high-intensity pulsed radiation can either stun or cause movement of the body. The effects of the pulsed radiation have not been confirmed by several studies that have non-thermal effects [13] [14].

1.5.4 Protective Measures for Radar

The purpose of protective measures is to improve the human exposure to RF radiation. When it is established that the radiation levels exceed those provided by the relevant directives, then, the protective measures are able to reduce the radiation exposure so as to be lower than the permitted levels. The protective measures, when necessary, divided into mechanical and administrative:

- Mechanical protective measures include safeguards in the operation of the radar (e.g. shutdown of the radar in case of mechanical damage to the antenna rotation system), electronic direction control of the radiation beam radar and shielding.
- The administrative measures include audible and visual alarms, warning signs, restricted access to areas of radar and restriction of the residence time, when necessary.

There are cases in which protective measures are not sufficient for the exposure levels to be below the recommended limits. Then, it is necessary to use personal protective equipment such as conductive clothing, gloves and safety shoes (Figure 1.3). Some points concerning this equipment are:

- The products that appear in trade in recent years "to protect vulnerable groups of the general population" are of questionable scientific merits. Their use should be avoided and prevented: There is no way in which it is necessary to use protective equipment from a person belonging to the general population.
- The material properties are dependent on the frequency of the radiation. It is therefore necessary to control the type of protection provided by the equipment in this radar operating frequency.
- Chose attention should be paid especially to safety eyewear, due to the fact that every metal part can act as an antenna and enhance local fields [13].

Figure 1.3 Personal Protective Equipment

Source: http://www.4ehsbyehs.com/protection-clothes

Sleeping bag for electro sensitive people
Source: http://shop.wireless-protection.org

Electromagnetic Protective Head Net
Source: http://emfclothing.com/en/

Electromagnetic Protective Maternity Belt (Pink)
Source: http://emfclothing.com/en/maternityclothing/

We can also take measures to protect ourselves against electromagnetic radiation by shielding the walls of our homes with special paint coatings grounded with special earthing pieces. We can use special curtains, self – adhesive films on window panes or special covers. (Figure 1.4).

Figure 1.4 Shielding Space

(Source: http://www.aktinovolia.com/protect.html)

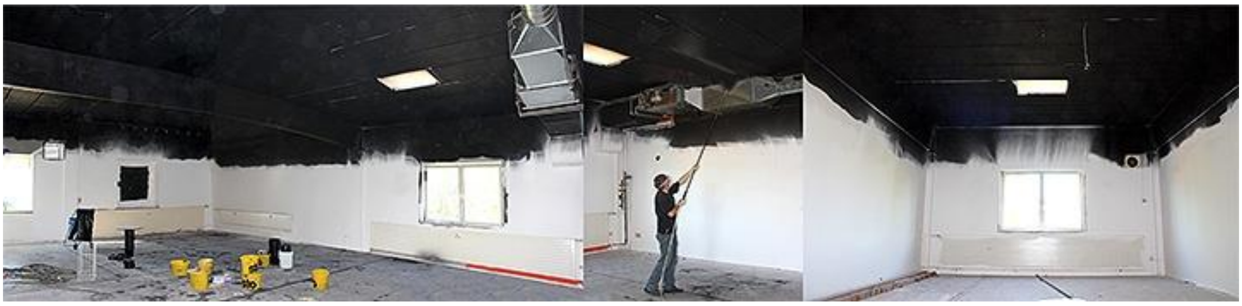

Chapter 2 –International Standards

2.1General Remarks

In the entire world, international organizations and countries have established permissible exposure limits for the general population and occupationally exposed population to non-ionizing electromagnetic radiation (NIR).

Most countries in Europe and others use exposure guidelines issued by the International Commission on Non-Ionizing Radiation Protection - ICNIRP. This non-governmental entity that is officially recognized by the World Health Organization (WHO), assesses the scientific results in the fields of epidemiology, medicine, biology, physics and engineering worldwide. The ICNIRP announces guidelines for proposed limits of exposure, which are reviewed and updated periodically, when necessary. The latest instructions of ICNIRP were published in 1998 and adopted by the CENELEC (Commission European de Normalization Electrotechnique) and European Council in drafting the present standard for exposure to electromagnetic fields. The ICNIRP guidelines are the basis for the Greek legislation for the protection of the public from exposure to electromagnetic RF radiation.

The ICNIRP guidelines for exposure to electromagnetic fields cover the frequency range of non ionizing radiation from 0Hz to 300GHz. They are based on extensive surveys which have been published in scientific literature. The acceptable limits of exposure have been established based on the results of short term intense exposure rather than long term exposure, because the available scientific information for long term effects of exposure to low intensity electromagnetic fields is considered insufficient for establishing quantitative limits. At frequencies higher than 1MHz, the implementation of permissible exposure limits aims at the avoidance of thermal effects of electromagnetic fields [9].

2.2 Responsible Organizations

The application of exposure directives to electromagnetic radiation is aimed at protecting humans from possible side effects of radiation on health. The papers published always collect the results of latest researches on the subject, usually selected with strict scientific criteria. Therefore, these instructions have great scientific value, but in order to be followed by everybody the legislation of a state must be incorporated, so as to take legal effect. Thus, the drafting of these laws is entrusted to international or national institutions with experience in security issues from radiation.

International and national organizations, which publish instructions limiting the exposure to electromagnetic radiation, are:

1) As mentioned above, the International Commission on Non-Ionizing Radiation Protection (ICNIRP). This committee is the successor of the International Non-Ionizing Radiation Committee (INIRC) of the International Radiation Protection Association (IRPA) and since 1992 is an independent, non-governmental organization, officially recognized by the World Health Organization (WHO) and the International Labour Organization (ILO). The latest ICNIRP guidelines were issued in 1998 [15].
2) The Commission of the European Union, which makes the guidelines for the protection of workers and the general public against the possible dangers of electromagnetic radiation exposure. The part of non-ionizing radiation was assigned to European Organization for Electrotechnical Standardization (CENELEC). In 1999 CENELEC adopted the ICNIRP guidelines for public exposure to non-ionizing radiation and published the relevant Directive (1999/519/EC, 12-07-1999).
3) The National Radiological Protection Board (NRPB). NRPB gives advice and information to equivalent government departments of the British government and is responsible for both ionizing and for non-ionizing radiation.
4) The American National Standards Institute (ANSI). Its corresponding part, which is responsible for issuing of exposure limits to radiation RF, collaborates with the Institute of Electrical and Electronic Engineers (IEEE). Also, in the United States, the Federal Communications Commission (FCC) enforces limits for both occupational exposure (in the workplace) and public exposure to Radiofrequency

Electromagnetic Fields. The allowable limits are variable, according to the frequency transmitted [16].

2.3 Standard Characteristics

2.3.1 Basic Restrictions and Reference Levels

The guidelines issued by the relevant organizations for dealing with effects on human health from exposure to electromagnetic radiation, include a clear distinction between the term "Basic restrictions" and "Reference levels". These basic restrictions and reference levels have developed following a thorough review of all published scientific literature. The criteria were only used for established effects to define these basic restrictions and reference levels. The occurrence of cancer from long term exposure to Extreme Low Frequencies (ELF) was not taken into consideration.

Basic restrictions: The adopted basic restrictions are based on the existence of documented effects on human health. The physical quantities that are used to define these restrictions differ depending on the frequency range. These physical quantities, are the current density (J), specific energy absorption rate (SAR), and power density (S). Only the power density can be readily measured in exposed individuals.

Reference levels: The reference levels are given in the exposure standards mainly for practical reasons. Since the quantities involved in Basic restrictions (e.g. SAR) are difficult to be measured. The reference levels are derived from the basic restrictions, with computational techniques or experimental results. Other reference levels include adverse indirect effects of exposure to EMFs. The physical quantities that are used to reference levels are: the electric field strength (E), the magnetic field strength (H), the magnetic flux density (B), power density (S) and current (I). Quantities that address perception and other indirect effects are contact current (IC) and, for pulsed fields, specific energy absorption (SA). These quantities can be easily measured with various instruments (e.g. spectrum analyzers with suitable receiving antennas, field meters with appropriate sensors).

Whenever an exposure to electromagnetic radiation occurs the measured or calculated value of the corresponding physical quantity can be compared to the appropriate the reference level. The compatibility of the measurements or calculations with the reference levels implies that basic restrictions are met. In contrast, the exceedance of reference levels does not imply automatic exceedance of the basic restrictions. This simply means that there should be a further check on the satisfaction of basic restrictions. This process is quite complex, it takes considerable time and further requires the extraction of the average value in various parts of the space on the site of measurements [15].

According to the guidelines of ICNIRP, a segregation of exposure limits of electromagnetic radiation has been proposed. Lower limits for the general population and higher for individuals involved professionally in the exposure spaces with electromagnetic radiation. This happens because the latter are aware of the risks and can take appropriate protective measures.

A safety factor has also been set for the establishment of basic restrictions. The safety factor is 10 for employees and 50 for the general public. It represents the uncertainty in the estimation of the limit occurrence of harmful health effects. E.g. for the specific absorption rate (SAR) the limit for negative effects is 4W/Kg (average value for the whole body) for frequencies from 100KHz to 10GHz. Therefore, the basic restriction for the employees is 0.4W/Kg and for the general public, 0.08W/Kg, calculated as an average value for the whole body and for a measurement period of six minutes [9].

The basic value for determining the quantity of thermal effects is the Specific Absorption Rate (SAR). Establishing limits of acceptable exposure by CENELEC and other standardization committees for whole body exposure to electromagnetic radiation, is based on preventing behavioral problems noticed in animals at exposure to low levels of radiation. The term "behavioral problems" refers to the tendency of animals to stop the execution of a complex cognitive function when exposed to specific electromagnetic energy levels. This thermal effect observed for the SAR equals to 4W/Kg body weight, and is calculated as an average value over the whole body.

For cases where the direct estimation of the power absorbed by the tissues is not possible, the ICNIRP defines reference levels corresponding to physical quantities, which can be easily measured, such as the electric or magnetic field strength or power density. The calculation of the reference fields by their respective basic restrictions has been made with the assumption of maximum coupling of the human body with the electromagnetic field (worst case) [9].

The limits (reference levels) proposed by the ICNIRP vary according to the frequency of the RF radiation. This is because the radio frequency energy absorption of the entire human body depends on the frequency of the radio frequency signal. The strictest limits for the whole body exposure correspond to the frequency range from 30MHz to300 MHz where the human body absorbs more RF energy because it is coordinated to the wavelength of the radiation. The amount of absorption depends on many factors, including the size and the height of the body. The maximum absorption frequency for the "typical man" is about 70MHz. For toller people the corresponding frequency has a lower value, while for children or babies can exceed 100MHz. For devices that affect only part of the human body with their radiation such as mobile phones, exposure limits are set only on the basis of SAR. Especially in the case of pulsed high frequency fields a basic restriction for the specific absorption SA has also been introduced [9].

Apart from the above basic restrictions, which are derived from the immediate biological effects of radiation, reference levels for contact current have also been adopted in order to avoid indirect effects such as an electric shock and burns due to contact with an object (usually metal) located in the electromagnetic field.

2.3.2 The issue of the limits for the general public

Different limits have been set for the general population and for workers. This is due to the fact that the occupationally exposed population consists of adult workers who, in general, are informed about the existence of electromagnetic fields and their effects. Employees are trained to be aware of possible risk and to take necessary precautions. In contrast, the general population consists of individuals of all ages with varying health conditions, which in many cases are not aware that they are exposed to electromagnetic fields. Moreover, workers are typically exposed only during the working day (usually 8 hours a day), while the general population may be exposed for up to 24 hours a day. These are the fundamental reasons for more stringent exposure restrictions for the general population comparing to the occupationally exposed population.

2.3.3 The average value of physical quantities

The term of the average value exists at all standards. The period used for the calculation of the mean value (basic restrictions and reference levels) is that of 6 min. It is obvious that the peak value set by the reference levels during the measurement time should always be considered, because at some of the standards peak allowable instantaneous values are set.

2.3.4 Exposure to multiple frequency radiation

In case of simultaneous exposure to fields of different frequencies, the possibility of accumulation effects of all fields should be considered and separate evaluations for thermal and electrical effects in the human body should take place.

2.4 European and Greek Legislation

2.4.1 Recommendation of the European Council (1999/519/EC)

In 1999 the European Union adopted the ICNIRP guidelines for public exposure to electromagnetic radiation and thus issued the Directive 199/519 /EC.

The basic restrictions for the general population in the RF - Microwave band are given in Table 2.1.

Table 2.1 The basic restrictions for the RF band

Frequencies (MHz)	Current density, rms (mA/m^2)	Whole-body average SAR (W/kg)	Localized SAR (head and trunk) (W/kg)	Localized SAR (limbs) (W/kg)	Power density (W/m^2)
0.1 – 10	f/500	0.08	2	4	-
10 – 1000	-	0.08	2	4	-
1000 – 300000	-	-	-	-	10

• f is the frequency in Hz.

Table 2.2 includes the reference levels for the fields with which the measurements are to be compared. Compliance with the reference levels ensures compliance with the basic restrictions.

Table 2.2 Reference levels in the radio frequency range

Frequencies	E-field strength, rms (E in V/m)	H-field strength, rms (H in A/m)	B-field, rms (B σε μT)	Equivalent plane wave power density (S_{eq} in W/m^2)
3-150 kHz	87	5	6.25	-
0.15-1 MHz	87	0.73/f	0.92/f	-
1-10 MHz	$87/f^{1/2}$	0.73/f	0.92/f	-
10-400 MHz	28	0.073	0.092	2
400-2000 MHz	$1.375\ f^{1/2}$	$0.0037\ f^{1/2}$	$0.0046\ f^{1/2}$	f/200
2-300 GHz	61	0.16	0.20	10

Although there is insufficient information on the relation between biological effects and peak value of pulsed signals for frequencies exceeding 10MHz, it is suggested that the average of S_{eq} throughout the pulse width should not exceed 1000 times the reference levels or intensities of fields should not exceed 32 times the reference levels for field strength. This applies to the Radar electromagnetic radiation measurements.

2.4.2 Safety Precautions for the Public in Greece

In Greece, the two laws related for the protection of the public from non-ionizing radiation is the Common Ministerial Decision no. 53571/3839, "Protection measures for the exposure of the general public to all land based antenna stations", Act No.1105/Vol. B/6-9-2000 and the law 3431/2006 " About electronic communications and other orders", vol. A, act no.13, Feb. 2006.

According to Common Ministerial Decision no. 53571/3839, the exposure on the freely accessible around the antenna areas must not exceed 80% of the limits set by the Recommendation of the European Council (1999/519/EC).

According to law 3431/2006 (which is the law in force to date) there should not be spaces accessible to the general population where exposure levels exceed the 70% of the limits set by ICNIRP around each building whose antenna emits electromagnetic radiation. Moreover, in case of installing the antenna construction closer than 300 meters from the perimeter of buildings of day nurseries, schools, nursing homes and hospitals, the public exposure levels are forbidden to exceed the 60% of the limits set by ICNIRP. Consequently, stricter limits than those set by the ICNIRP are applied in Greece. Table 2.3 contains the reference levels for thermal effects reduced by the factor of 70%.

Table 2.3 Reference levels for thermal effects by the factor of 70%

Frequencies	E-field strength, rms (E in V/m)	H-field strength, rms (H in A/m)	B-field, rms (B in μT)	Equivalent plane wave power density (S_{eq} in W/m^2)
100kHz – 10 MHz	$72{,}8 / \sqrt{f}$	$0{,}61 / f$	$0{,}77 / f$	-
10 – 400 MHz	23,4	0,061	0,077	1,4
400 – 2000 MHz	$1{,}15 . \sqrt{f}$	$0{,}0031 \bullet \sqrt{f}$	$0{,}0038 \bullet \sqrt{f}$	$f / 286$
2 – 300 GHz	51	0,134	0,167	7

Table 2.4 contains the reference levels for thermal effects reduced by the factor of 60%.

Table 2.4 Reference levels for thermal effects by the factor of 60%

Frequencies	E-field strength, rms (E inV/m)	H-field strength, rms (H in A/m)	B-field, rms (B in μT)	Equivalent plane wave power density (S_{eq} in W/m^2)
100kHz – 10 MHz	$67,3/\sqrt{f}$	$0,565 / f$	$0,71 / f$	-
10 – 400 MHz	21,7	0,0565	0,071	1,2
400 – 2000 MHz	$1,065.\sqrt{f}$	$0,00287 \bullet \sqrt{f}$	$0,00356 \bullet \sqrt{f}$	$f / 333$
2 – 300 GHz	47,2	0,124	0,155	6

- f is the frequency in MHz.

In Greece, the Greek Atomic Energy Commission (EEAE) is the competent regulatory authority for the control, regulation and supervision of compliance with the limits of public exposure to electromagnetic radiation. The tests for measuring the radiation are carried out by the EEAE or its authorized bodies.

In this work, measurements for the primary Air traffic control radar at the airport of Heraklion, where the operating frequency is 2840 MHz or 2760 MHz have been made. So, the reference levels with which our measurements are compared are shown in table 2.5:

Table 2.5 Reference levels for thermal effects by the factor of 60%

Frequencies	E-field strength, rms (E in V/m)	H-field strength, rms (H in A/m)	B-field, rms (B in μT)	Equivalent plane wave power density (S_{eq} in W/m^2)
2 – 300 GHz	47,2	0,124	0,155	6

Chapter 3 –Basic Principles of Radar Operation

3.1 RADAR – Introduction- History

The RADAR is a basic electronic system of electromagnetic detection which identifies and monitors either movable or immovable targets, over long distances, which are not visible to the human eye.

The device name is derived from the initials of the English words "RAdar Detection And Ranging», Radiation Detection and Range Finder. That is a device that works with electromagnetic waves (Radio), detects objects (Detection) and informs us about their position (Ranging).

In 1886-1888 the German physicist Hertz experimentally found reflection and scattering of electromagnetic waves on conductive objects. Similar surveys were made in 1897 by the Russian scientist Popov. The first Radar was experimentally constructed in 1903-1904 by the German engineer Hulsmeyer.

In 1935 the British Watt and Wilkins made a historic experiment in a village in England and achieved early detection of enemy aircraft at a great distance well before their visual identification, using a shortwave transmitter of the BBC, at 6 MHz, with a power of 10 KW. In 1939 the British placed many Radar stations with a frequency of 60 MHz as an early warning system along the coasts of the English Channel. Before the bombing of the Pearl Harbor base in Hawaii Japanese aircraft were identified by the survey radar based in Honolulu, but had been ignored.

Lighter and more accurate radars were developed with the discovery of the first microwave tube magnetron (3 GHz, λ = 10 cm, with a power pulse of 10 KW), and soon (1942) the first microwave radar (S-band, λ = 10 cm) with rotating antenna was developed.

In 1958 the US invented the 3D search radar-tracking systems and in 1960 the first American pulse compression radar (pulse compression) was constructed.

More over two types of radar were developed. Initially, the CW radar (continuous transmission) and then pulse radars, which are the most popular and are found in many applications today.

There are many radar types depending on the features that want them to perform. Some of them are: the research radar / surveillance, fire management radar (fire control), air traffic control radars, approach radars at airports, ground controlled approach, directional projectiles, mapping (aerial photography), shipping, Doppler, meteorology, measurement speed, surveillance / monitoring satellites, etc [17].

3.2 The basic principles of Radar operation

The radar is used to gather information about a target. Thus, the position, the velocity, the direction, the shape, the identity or simply the presence of an object can be found. This is done by processing the radio frequency signal (RF) or microwave that is reflected in the case of primary radar, or by a transmitted response in the case of the secondary radar (Figure 3.1).

The transmission of the question signal and the reception of the response are carried out from the same antenna of the radar system. This basic process is described by the radar equation. The signal power at the radar receiver is directly proportional to the transmitted power, antenna gain (or aperture size), and radar cross section (RCS) (the degree to which an object reflects the radar signal) and indirectly proportional to the fourth power of the distance to the target. There is a high attenuation in the path of the signal until it reaches the receiver, and thus high transmission power is required. This is not easy because there are practical problems such as heat, voltage breakdown, system size and cost [18].

Figure 3.1 Radar Principle

Source:http://www.radartutorial.eu/01.basics

3.3.1 Pulse Characteristics

The pulsed radar is the basic type of radar used. The aim is to identify and determine the position of various targets (ships, aircraft, etc.) based on the transmission and reception of a series of radio pulses of short duration. The envelope of the pulses is rectangular with a fixed width and very small rise and fall times. Figure 3.2 shows the pulsed radar signal.

Figure 3.2 Pulsed Radar Signal

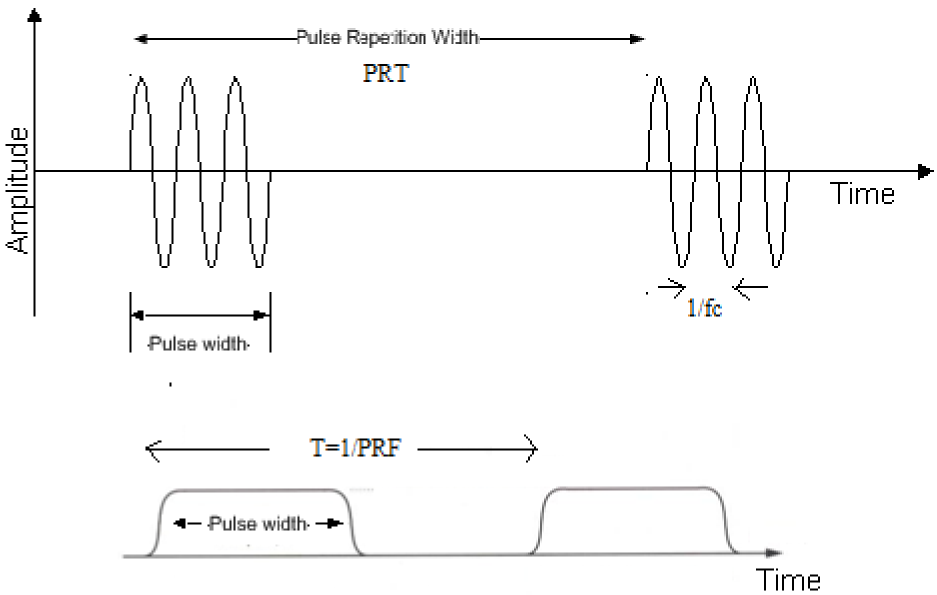

The basic characteristics of the pulsed radar signal are:

1) Sine carrier with frequency (carrier frequency) fc of radio pulses.
2) Maximum power output (peak power), Pt. The product of this power by the duration of the pulse gives us the energy per pulse.
3) Average radiated power (average power), Pav. It is evenly distributed over power pulse across the pulse repetition period. Pulse repetition period (Pulse Repetition Time), which determines the time between two successive pulses. The inverse of this quantity is called the pulse repetition frequency (Pulse Repetition Frequency), PRF, which determines the number of pulses emitted per second and the maximum unambiguous range to the target.
4) Duty cycle is equal to the ratio PW/PRT and it is the percentage of the duration of the pulse emission, to the total length of the repetition period T of pulses.
5) Energy emitted pulse (pulse energy), which is equal to $E = P_t \bullet PW$
6) Antenna rotation rate expresses the turns of the antenna per minute rpm.
7) Pulse Width is denoted by PW or τ. Pulse width determines the spatial resolution of the radar. The pulses must be less than the time it takes the signal to travel between the target details. Otherwise, the pulses overlap the receiver. The pulse width and pulse shape also determine the range of the radar signal. Reducing the pulse width increases the bandwidth of the signal. But there is also greater noise in the receiver, thereby reducing its sensitivity.

Short pulses with a low repetition rate maximize resolution and unambiguous range and high pulse power maximizes the radar's range in distance. But there are practical and technical problems to generate such pulses, for example reducing the lifetime of materials. For this reason used pulse compression techniques and complex waveforms [18] are used.

Figure 3.3 Power spectrum of the Heraklion PSR radar [19]**.**

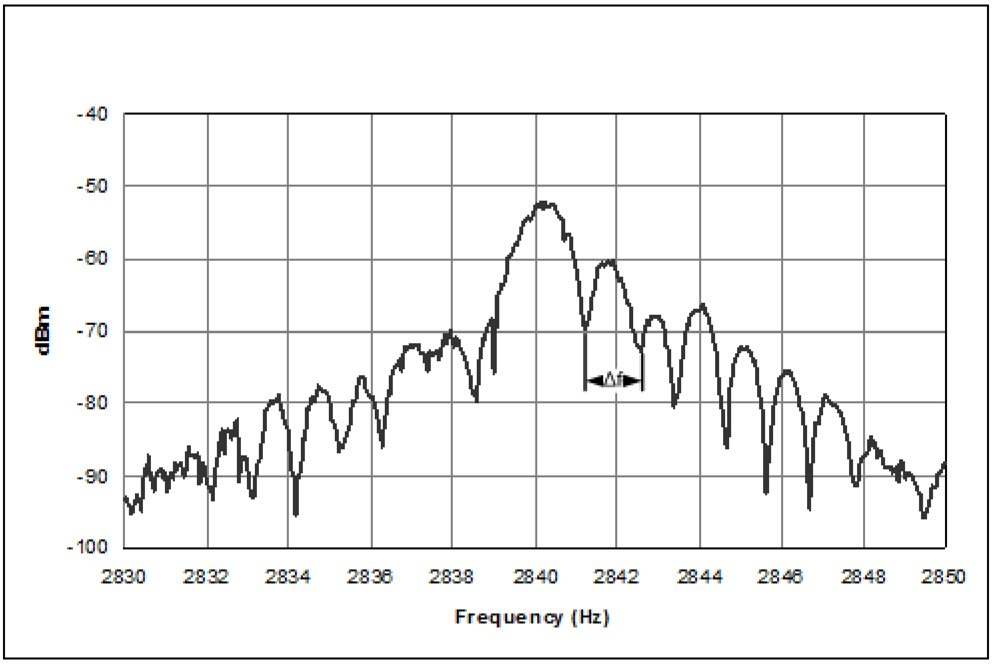

Another characteristic of the radar is the total time in which an object is located within the main lobe of the radar and is called time on the target (Time On Target- T_{OT}) and is equal to

$$T_{oT} = \frac{\Delta_{\Phi}}{360^0} t_{rot}$$

where: Δφ is the beamwidth angle of the radar antenna and t_{rot} is the time it takes one radar antenna rotation to complete.

3.3.2 Pulse Compression

The ideal impulse radar system would be one that could emit pulses of very short duration and high power. So we have: good range resolution, large detection distances (improved SNR) and high resistance to interference. Such a system however presents many technical difficulties and for that reason pulse compression techniques are applied.

The idea is to modulate the transmitted pulses that after the reflection of the target and its return to the receiver a separation can be made even if they are separated by a distance less than the range resolution.

For compressing the pulses different techniques are used such as: linear FM sweep, binary phase coding (e.g., Barker codes), or polyphase codes (e.g., Costas codes). The most common is the linear frequency modulation in which the pulse frequency is varied linearly with time. This technique is called "chirp" because it reminds a bird’s chirp and often occurs with the term "chirp modulation".

For the compression of the pulses matched filters are used. The matching filter function can be achieved digitally using the cross-correlation function to compare the received pulse with the transmitted pulse.

The sliding frequency due to the Doppler effect is one of the most basic problems in frequency modulation techniques [17] [18].

3.3.3 Doppler Frequency

It is known from the theory of Wave Motion, that when there is a relative motion of the observer and the source wave (acoustic or electromagnetic) of fixed frequency f, then the frequency of the waves received by the observer is different from that of the source (Doppler effect). At the operation of radar this happens because most of the targets of interest move and they cause the frequency of the returned signal to shift higher if the target moves toward the radar and lower, if the target moves away. Doppler frequency shift can reduce the sensitivity of location detection.

3.3.4 The Radar Range Equation

The radar range equation describes the important performance variables of Radar and provides a basis for understanding the measurements that are made to ensure optimal performance.

We consider that a radar antenna emits a signal with Pt peak power in the direction of the target which is at a distance R and has radio cross section, RCS, σ. The transmit antenna is directional with a gain Gτ. So, the power density P_T which reaches the target position is (figure 3.4):

$$P_T = \frac{P_t}{4 \cdot \pi \cdot R^2} \cdot G\tau$$

Figure 3.4 Transmitted and reflected power returned to the radar [18]**.**

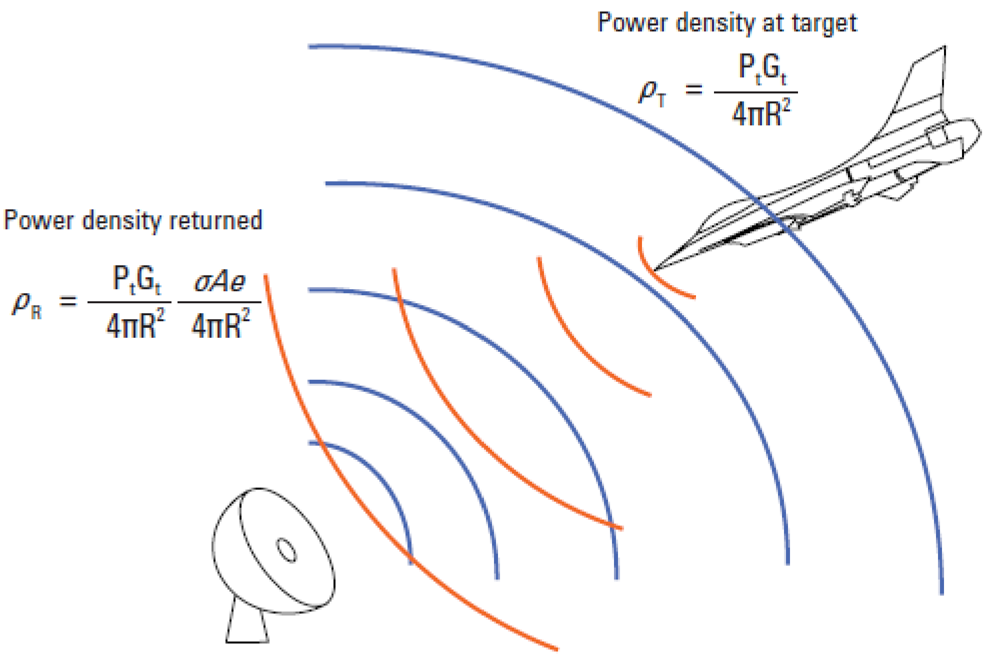

RCS (Radar Cross Section) of a target is defined as an imaginary surface at the target, and when it isotropically scatters the entire incident to this power, then the same echo as the real target is produced on the radar. It is measured in surface units (m^2), it is defined as 4π by the ratio of the power per unit solid angle $\left(\frac{Watt}{sterad}\right)$ and it is reflected from the target back to the source.

The signal power received at the receiver in watts is equal to:

$$S = \frac{P_t \cdot G_T^{\,2} \cdot \sigma \cdot A_e}{(4\pi) \cdot R^4}$$

where:

S = signal power received at the receiver in watts

P_t = transmitted power in watts

G_T = gain of transmit antenna

σ = RCS of target in square meters

R = radius or distance to the target in meters

Ae= effective area of the receive antenna square meters

The antenna theory allows us to relate the gain of an antenna to its effective area as:

$$A_e = \frac{G_R \cdot \lambda^2}{(4\pi)}$$

where:

G_R = gain of the receive antenna

λ = wavelength of radar signal in meters

So, the equation for the received signal power can now be simplified.

$$S = \frac{P_t \cdot G^2 \cdot \sigma \cdot \lambda^2}{(4\pi)^3 \cdot R^4}$$

where:

S = signal power received at the receiver in watts

P_t = transmitted power in watts

G = antenna gain (assume same antenna for transmit and receive)

σ = RCS of target in square meters

λ = wavelength of radar signal in meters

R = radius or distance to the target in meters

The analysis of the signal takes place in the receiver and the extracted information is affected mostly by the noise. For radar systems the noise can come either from outside or from the receiving system itself.

The random movements of electrons in the resistive input sections of a receiver cause thermal noise (thermal or Johnson noise). The value is proportional to the temperature of resistance portions and the bandwidth B of the operating frequency band of the receiver (in particular the bandwidth of the IF amplifier). So,

N=kTBn

where:

N = noise power in watts

k = Boltzmann’s constant (1.38 x 10-23 Joules/degree Kelvin)

T = temperature in degrees Kelvin

Bn = system noise bandwidth

The magnitude characterizing the performance of a radar is known as MDS (Minimum Detectable Signal) or receiver sensitivity of the receiver. Therefore:

$$S_{\min} = k \cdot To \cdot Bn \cdot F_n \cdot \left(\frac{S_o}{N_o} \right)_{\min} = \frac{Pt G^2 \lambda^2 \sigma}{(4\pi)^3 R_{\max}^4}$$

The maximum detection distance of the radar is:

$$R_{\max} = \left[\frac{Pt \cdot G^2 \cdot \sigma \cdot \lambda^2 \cdot E_i(n)}{(4\pi)^3 \cdot k \cdot To \cdot F_n \cdot Bn \cdot L_T \cdot L_R \cdot \left(S_o / N_o \right)_{\min}} \right]^{1/4}$$

where:

LT = losses in the transmitter path

LR = losses in the receive path

Ei(n) = integration efficiency factor (The process associated with the sum of returned pulses to improve the ability of the detect of the radar, is called pulse integration. The integration efficiency factor Ei (n) is lower than 1).

R = maximum distance in meters

P_t = transmit power in dBW

G = antenna gain in dB

λ = wavelength of radar signal in meters

σ = RCS of target measured in dBsm, or dB relative to a square meter

FN = noise figure (Noise figure = noise factor converted to dB)

S/N = min signal –to-noise ratio required by receiver processing functions detect the signal in dB.

$$E_i(n) = \frac{\left(S/N\right)_1}{n\left(S/N\right)_n}$$

where n is the number of pulses of equal width completed and $\left(S/N\right)_1$ is the signal to noise ratio of a single pulse needed to achieve the specific detection probability. The $\left(S/N\right)_n$ is the value of the signal to noise ratio, when are completed n pulses, in order to achieve the same value detection probability and false alarm in the event of a single pulse.

3.3.5 Radar Block Diagram

Figure 3.5 shows a Radar block diagram of the transmitter and receiver sections. The callouts indicate the location of key variables within the radar equation.

Figure 3.5 Radar Block Diagram [18]**.**

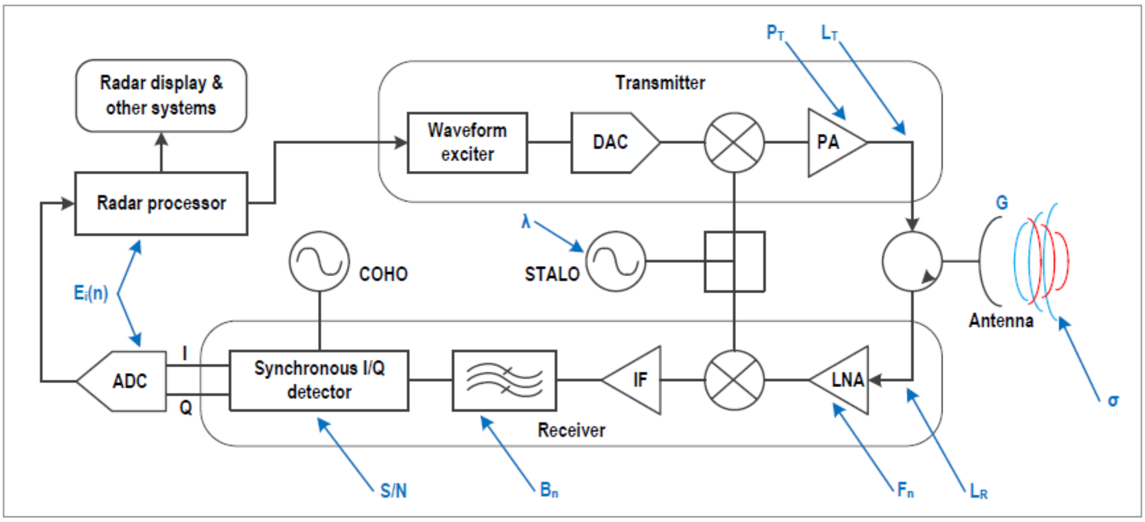

3.4 RADAR Measurements

3.4.1 Power and Spectrum measurements

Measurements on various parameters of radar can be made. Thus, the average power which is the power that is integrated over the complete time waveform of the radar can be measured. The peak power, which is the maximum instantaneous power can also be measured. Other parameters that can be measured are the duty cycle, pulse width, PRF, and rise and fall times as shown in Figure 3.6.

Figure 3.6 Pulse Parameters [18]**.**

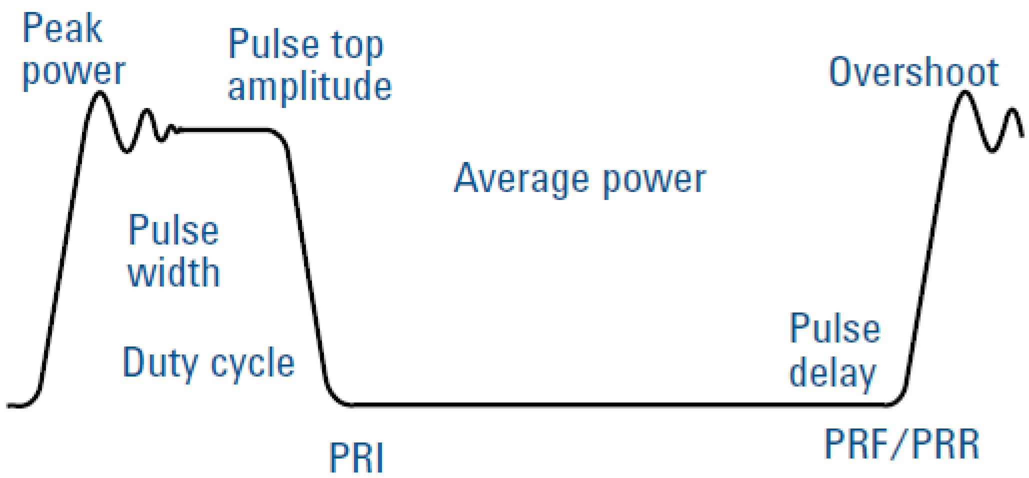

Besides the measurements of power, the spectrum shape is also required to be measured, in order to verify that the radar system operates properly. If, for example, we have an asymmetric spectrum, then this means that the radar operates wrong. As a result, the radar can squander energy transmission or cause interference to other systems.

There are several ways to measure radar power, the characteristics of the pulse and spectrum. This can be done by using a power meter, a spectrum analyzer, or vector signal analyzer. Because each instrument has both advantages and limitations, the best option is determined by the objectives of measurement and limitations of radar. For example, the RF and microwave instruments are limited in both the amount of average power and the amount of peak power that can be inserted without damaging the instrument.

3.4.2 Calculating Distances from the Radar

Based on the dimensions of the antenna of the radar and the wavelength of the transmitted signal, the distances are calculated according to the boundaries between the areas of the field (near, intermediate, or far) [20]. Specifically, the area in front of the radar and along the major axis will have the following sub-areas Figure 3.7:

Figure 3.7 Near and Far field areas of the Radar

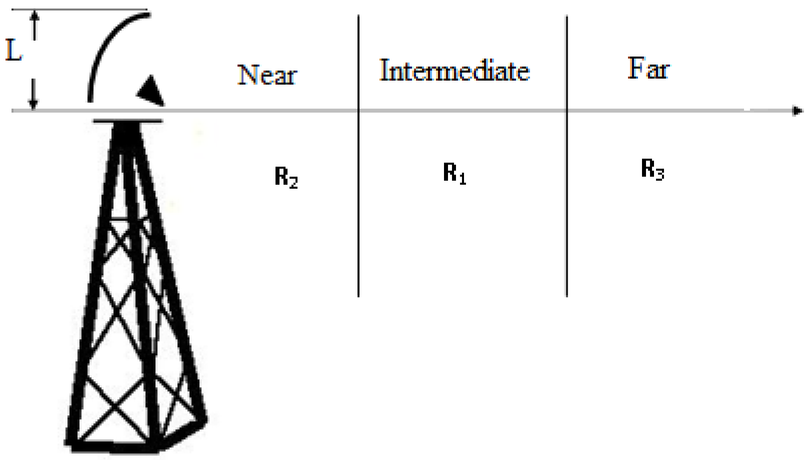

Near Field: Rayleigh Distance (R_2)

This region extends from the surface of the radar antenna to the distance:

$$R_2 = \frac{L_2^2}{2 \cdot \lambda}$$

where: L_2 is the vertical dimension of the antenna and the λ the wavelength.

The emitted power in this area is mainly restricted within an elliptical cylinder which is based on the radar antenna.

For Heraklion PSR Radar we have:
$L_2 = 3.15$m and $\lambda = 0.106$ m. So,

$$R_2 \cong 47 \text{ m}$$

Intermediate Field: Rayleigh Distance (R_1)

The intermediate area is determined by the distance R_2 and the distance R_1, which is defined by the formula:

$$R_1 = \frac{L_1^2}{2 \cdot \lambda}$$

where: L_1 is the horizontal dimension of the antenna.

In this region we have energy dispersal in the vertical plane (axis L2), and not in the horizontal plane (axis L1). In the intermediate range the power density varies inversely as the distance d from the radar.

For Heraklion PSR Radar we have:
L_1 = 5,5m and λ = 0.106 m. So,

$$R_2 \cong 143 \text{ m}$$

Far Field: Rayleigh Distance (R_3)

In the far field the power emitted in all directions, according to the radiation pattern of the antenna and the power density is inversely proportional to the square of the distance d.

It is defined by the formula:

$$R_3 = \frac{2 \cdot L_1^2}{\lambda}$$

For Heraklion PSR Radar we have:
L_1 = 5,5m and λ = 0.106 m. So,

$$R_3 = 571 \text{ m.}$$

3.4.3 Calculation of Power Density

Far Field:

In the far field and over the distance R_3, the average power density on the axis of maximum gain of the antenna and rotating radar, is given by the formula:

$$P_1 = \frac{P_{av} \cdot G}{4\pi d^2} \cdot \frac{\beta}{360}$$

where:

Pav: is the average radiated power

G: is the antenna gain

β: is the half power angle in degrees in the horizontal plane (azimuth).

Intermediate Field:

In the intermediate field, the average power density on the axis of maximum gain of the antenna and rotating radar is given by the formula:

$$P = \frac{P_{av} \cdot G}{2\pi R_1^2} \cdot \frac{L_1}{2\pi d} \cdot \frac{R_1}{d}$$

Near Field:

In the near field, the average power density on the axis of maximum gain of the antenna and rotating radar is given by the formula:

$$P = \frac{P_{av} \cdot G}{2\pi R_1^2} \cdot \frac{L_1}{2\pi d} \cdot \frac{R_1}{R_2}$$

Chapter 4 –Measurements of Pulsed Radar

4.1 Pulse Power Measurements with Power Meter

As mentioned in a previous chapter the Radar works by emitting a beam, which scans the area where there are targets of interest. A target is detected when it is in the line of sight of the transmitting antenna. So, the echo of the target is returned to the radar receiver and if it is too strong and above the noise level, the radar considers it as a target.

Some parameters of the radar such as the transmitted power and the characteristics of the pulse, can significantly affect the performance of the radar system. For this reason, the measurements of such characteristics need to be done correctly by using proper tools and devices.

The most common, simple and inexpensive way to measure pulse power is the power meter. With the power meter we can measure average power, peak power and other features of pulse. The power meter uses the power sensors for the measurements. The power sensors convert the high frequency current to a DC or low frequency signal so that the meter can make measurements and relate to a certain RF or microwave power level. There are three main types of sensors: the thermistors, thermocouples, and diode detectors. The thermistor sensors are based on the function of a balanced Wheatstone bridge. The disadvantage of these sensors is their sensitivity to changes in temperature. The thermocouple sensors detect changes in voltage, which are the result of temperature changes caused by incident RF power on the thermoelectric element. The thermistor and thermocouple sensors can be used for measuring average power but cannot be used for the direct measurement of peak power. The diode – based sensors rectify the signal. Thus RF voltage is rectified and converted into DC voltage at the diode. The diode- based sensors have good sensitivity, and thus can make measurements of very low power, such as -70 dB. Thermocouples can also be damaged more easily than diodes at high power levels [18] [21] .

The use of an **average power meter** for pulse power measurement is the most simple and cheap solution, since both the meter and the sensors are low cost. The average power meter can measure the strength of the pulse when the duty cycle of the pulse is known. However, it cannot readily determine peak power or other characteristics of the pulse. The measurements taken by the average power meter will be accurate when the pulse signal is an ideal signal. Usually, perfect square signals cannot be transmitted and always, an overshoot and a relative rise and fall time will be different from that of purely rectangular pulse.

The **peak power meter** can make pulse measurements and peak power directly and provides information in time domain with triggering and gating functions. This way more simple analysis of pulsed RF radar signals can be conducted.

Another way to make radar measurements is to use **Vector Signal Analyzer** (VSA). Besides measuring the power of the signal it is sometimes necessary to determine the modulation, the measurement of phase or some transient characteristics of the radar. So, a VSA captures phase and magnitude information of the measured signal and uses this information to perform more advanced analysis. Its operation is based on the tuning to a specific frequency, the conditioning of the signal, the down converting, the digitizing, and the processing of the signal. A VSA shows the effects on the time, frequency and modulation domain. An important disadvantage of VSA is the analysis bandwidth (or information bandwidth or Fast Fourier Transform (FFT) bandwidth). To properly analyze a signal, all the signal power must be contained within the instrument analysis bandwidth [22].

4.2 Pulsed Radar Measurements with Spectrum Analyzer

A different way to make Radar measurements is by Signal/Spectrum analyzer (SA). With the SA, besides measuring the power, we can also obtain information about the frequency content. Thus, we can see the spectrum of the transmitted pulse on the SA screen. This is very important because a non-symmetric spectrum will show us that the radar does not work properly and an error exists in its various component parts. Also from the spectrum of the pulse some characteristics of the pulse can be calculated, such as the pulse width and the Pulse Repetition Frequency (PRF).

Measuring Pulsed Radar with a spectrum analyzer is not an easy process. There are several analyzer modes of operation which depend upon the values of the resolution bandwidth (RBW) of the spectrum analyzer. Measuring a pulse signal with a spectrum analyzer is difficult but it becomes more complicated when low Duty Cycle pulsed signal is measured such as, the Radar signal. In addition, spectrum analyzers, which work with fast Fourier transform (FFT) function, have different behavior during Radar measurement.

In this work pulsed radar signal measurements have been performed with the help of a spectrum analyzer. This method of electromagnetic field measurements is narrowband measurements. Signal power was measured and its spectrum was illustrated. The measurements were made by using the appropriate equipment of the Non-Ionizing Radiation Laboratory of TEI of Crete. The remote communication with the spectrum analyzer and the processing of the measurements were performed with the development of the appropriate software in the Matlab environment.

4.3 Broadband and Narrowband Measurements

The best known methods of measurement of electromagnetic fields are the broadband measurements and narrowband measurements. When the greater part of the spectrum of the signal measured is within the bandwidth of the measuring device then we have broadband measurements. Usually the broadband measurements are made with a field meter with the appropriate broadband electric or magnetic field probe. When the central spectral component is contained within the passband of the IF filter, then we have Narrowband measurements. Such measurements are made with a Spectrum Analyzer, where IF bandwidth is reported as resolution bandwidth (RBW) (Figure 4.1). The continuous wave (CW) signals are a specific case of narrowband signals, since they consist of only one spectral line which is within the passband of the intermediate frequency (IF) filter [23].

When broadband measurements are performed, the process is quick and the equipment is simple. But the sources cannot be identified neither can their contribution to the whole emission be determined when there are a lot of transmission sources. Another disadvantage to this type of measurement is when their results are compared to the reference levels of exposure to electromagnetic fields in order to assess compliance with these levels. Since the reference levels are dependent on the frequency, we cannot make an accurate assessment of compliance with them, since there is no information for the frequency of the measured field.

On the other hand, with narrowband measurements the process takes a long time to complete, and requires more complex equipment. To make sure that the measurements obtained in this way are correct, we should introduce the appropriate settings in the analyzer. In this way, we can identify the emitting source in each position and we can determine its contribution to the total electromagnetic field exposure.

Figure 4.1 Broadband and Narrowband detection

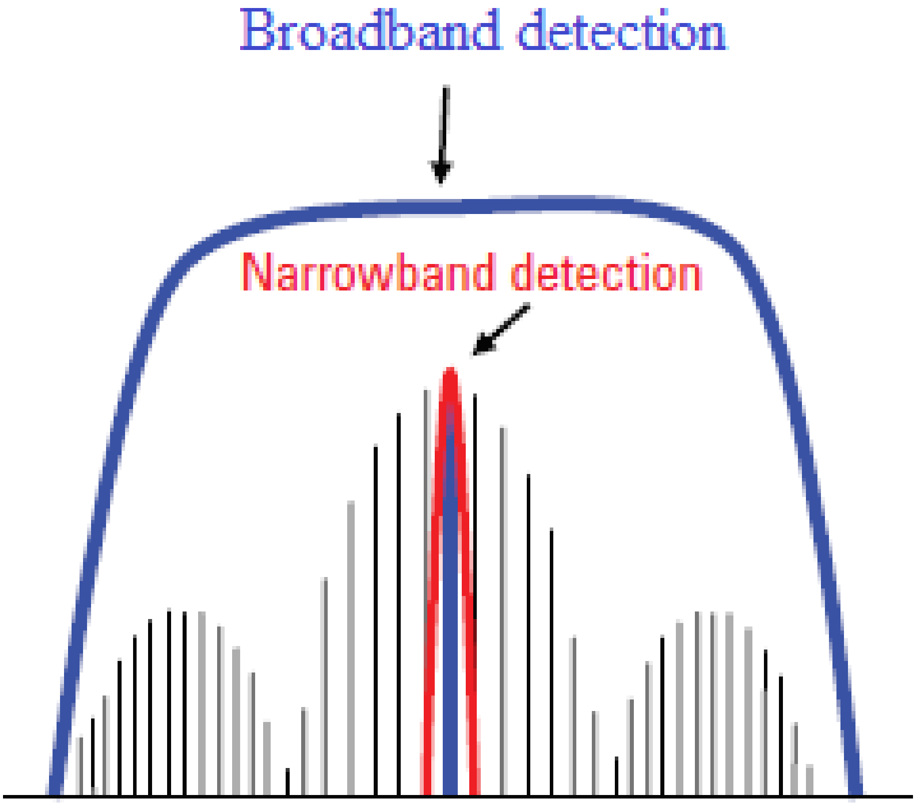

4.4 Shape of the Pulsed Spectrum

The spectrum analyzer is an electronic device that can measure the characteristics of radar pulse. The characteristics of the radar are: operating frequency, duration and pulse repetition frequency, the bandwidth, the duty cycle, the average power and peak power. When the signal of a pulsed radar enters the spectrum analyzer, the spectral content is displayed on the screen. The spectrum of a pulsed signal has the form of a sinc signal with a main lobe and side lobes. This comes from the multiplication of a continuous wave signal with a pulse waveform in the time domain. The spectrum of the pulsed radar is mathematically analyzed by applying Fourier transformation to a rectangular waveform, transiting it to the frequency domain.

As it can be seen in Figure 4.2, the pulse width and the PRF of signal define the characteristics of the basic pulsed spectrum. As the pulse width narrows, the width of the spectrum and side lobes expands. The PRF pulse - RF waveform determines the distance between each spectral component.

Figure 4.2 Pulsed Spectrum [18]

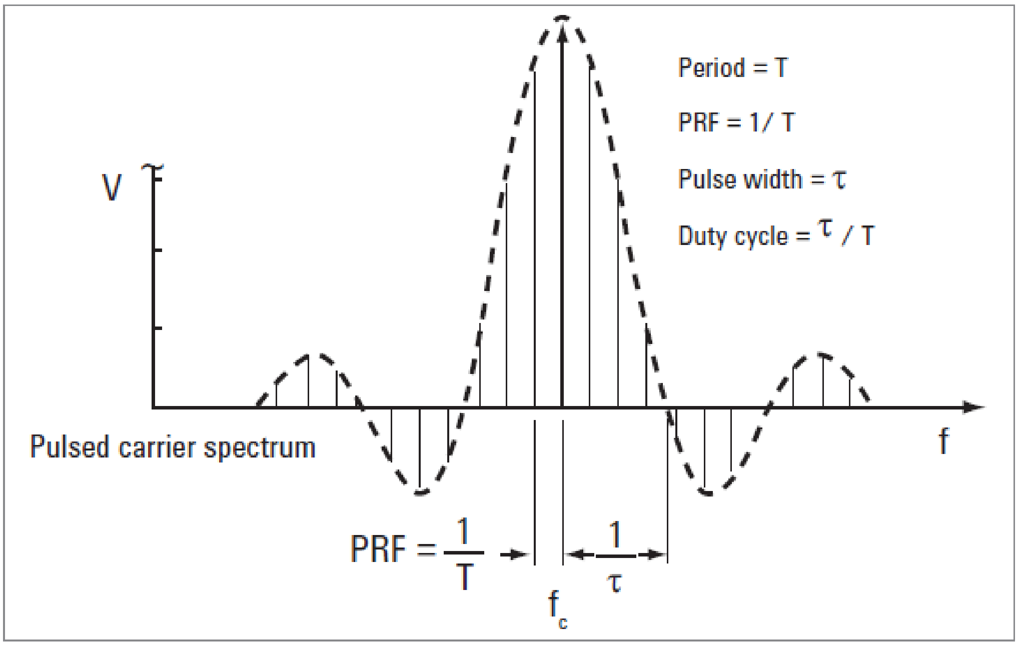

4.5 Pulsed Radar Measurements with Swept Spectrum Analyzer

In the report of Agilent Application Note [18] for Radar Measurements the methods of pulsed radar measurements with swept spectrum analyzers are described and analyzed in detail. Also, in this document some built-in functions and features which modern spectrum analyzers can support that can simplify and enrich Radar measurements today, are presented.

Conventional spectrum analyzers are based on analog swept super-heterodyne architectures. Newer analyzers use digital swept architecture, so they have better data on processing speed and more accuracy.

In order to have correct measurements with a spectrum analyzer we have to apply the correct settings on it. The analyzer parameters which must give the appropriate values to have reliable measurements are: Frequency Span (SPAN), Center Frequency (CF), Resolution Bandwidth (RBW), Sweep Time (SWP) and Video Filter Bandwidth (VBW) [24] [25].

Frequency Span (SPAN): Span is the frequency range across the 10 major horizontal divisions of the display of the spectrum analyzer. So, if we set Span = 20MHz then each of 10 divisions are 2 MHz. In **Zero Span**, the analyzer no longer sweeps across a spectrum. The analyzer is "tuned" to the center frequency and the signal presence in the RBW filter is continuously displayed.

Center Frequency (CF): The center frequency is the frequency of the transmission of the signal which can appear on the centerline of the display grid and is around the carrier frequency.

Resolution Bandwidth (RBW): The RBW is the frequency bandwidth of 3 dB IF analyzer filter. This filter determines the resolution bandwidth. When RBW is equal to half the width of the main lobe of the pulse spectrum, the amplitude that appears on the screen of the analyzer is practically equal to the peak amplitude of the signal. This range, according to the Fourier analysis, is equal to 1/ t_{eff}, where t_{eff} is the duration of an equivalent square wave of the same width and power of the pulse applied to the input of the analyzer.

Sweep Time (SWP): Sweep Time is the duration of a sweep and should be greater than the rotation period of the radar.

Video Filter Bandwidth (VBW): The Video Filter Bandwidth is the range of the video filter which is a post - detection filter. It is used to reduce the noise in the displayed spectrum and to make the low level signals more visible.

The swept spectrum analyzers have three primary modes of operation: line spectrum, pulse spectrum, and zero span.

Line Spectrum mode

When the relation **RBW<0.3*PRF** is true, the displayed spectrum is known as spectrum lines. The spectrum consists of spectral components (lines) which are spaced with multiples of the PRF. The figure 4.3 shows the line spectrum.

Figure 4.3 Line Spectrum [18]

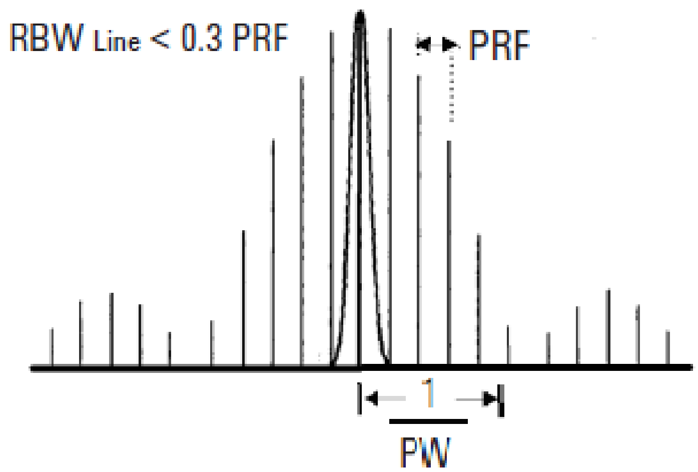

The Line spectrum has two characteristics at the frequency domain: A) the spacing between lines on the display will NOT change when the analyzer sweep time is changed. B) the amplitude of each line will not change when the RBW is changed as long as RBW remains below the PRF.

When the line spectrum is formed the power cannot be easily measured because the signal level is distributed into its spectral components. The duty cycle can be calculated from the line spectrum because the distance between the spectral lines is equal to the PRF and the distance between the nulls of the spectrum's sinc function shape is equal to the inverse of the pulse width.

Pulse Spectrum mode

When **RBW≥PRF**, the IF analyzer filter allows more spectral lines to pass and as a result the envelope of the received signal is illustrated. The illustration of the spectrum in the specific form is called pulse spectrum. The completion of energy from all the received spectral lines which pass simultaneously the IF filter is performed in the pulse spectrum mode. This means that the maximum displayed level of the signal depends on the RBW and thus it will be considered as a correction factor which depends on the signal characteristics and the RBW. This factor should be taken into account at the measured value to calculate the actual value of the received power. The correction factor is given by the relation:

$$a_p = 20log_{10}(\tau_{eff} * B_{imp)}\ [dB]$$

and called desensitization factor.

B_{imp} is the equivalent width of the IF bandwidth when considered an ideal, rectangular shaped filter with a pulse response equivalent to the actual filter with the 3 dB bandwidth RBW. As B_{imp} is not the same as the 3 dB RBW, a factor K is introduced. We have:

$$K = \frac{B_{imp}}{RBW}$$

So, the α_p is given by:

$$a_p = 20\log_{10}(\tau_{eff} \cdot K \cdot RBW)\ [\mathrm{dB}]$$

where t_{eff} is the pulse width in seconds and RBW is the resolution bandwidth in Hz [25]. The value of K is given by the manufacturing company. But for more precise determination of the value of the factor K, laboratory determination of its value can be found as happened at work [26]. For this purpose a pulse signal of known characteristics produced by a generator was used. The K depends strongly on *RBW*, and it does not have a constant value. In work [27] laboratory determination of the value of the α_p took place according to the specific characteristics of the signal detection and measuring instruments.

Therefore, the corrected peak power value will be given by subtracting the desensitization factor from the measured peak power value in spectrum analyzer.

To obtain correct results after applying the above relationship we should also apply certain conditions related to the operation of the spectrum analyzer in the pulse spectrum mode and the characteristics of the measurement pulse signal in order to find the right characteristics of the radar signal. These conditions are summarized in the following relationships [18] [25]:

$$RB < \frac{0.2}{\tau_{eff}}, \quad RB > PRF, \quad ST \geq \frac{10}{PRF} \quad \text{and} \quad 1.7 \cdot PRF < RB < \frac{0.1}{\tau_{eff}}$$

In pulse-spectrum mode the form of spectrum will change if the sweep time changes.

The pulse spectrum mode is most appropriate for controlling the parameters of radar rather than the line spectrum mode. This is because it gives a stronger signal, allows better scanning and gives information on both the spectrum and the PRF of pulses.

Zero-span mode

Not only can measurements in the frequency domain be performed, but also in the time domain. This can be done with zero Span mode. In this mode at the spectrum analyzer “0 Hz” is entered into the Span value. This way the SA would stop sweeping the LO and the analog resolution bandwidth filter would essentially be "parked" at a fixed frequency [28]. Then on the screen of SA, the power will not be displayed as a function of frequency but the as a function of the time and besides that, we can see the Pulse envelope. The SAs currently used have various trigger signals so as to provide a stable display to the modes. In the Zero Span mode the spectrum analyzer must be set to a RBW and VBW value wide enough to settle within the pulse width and the sweep time must be the lower possible value.

With the Zero Span mode we can easily measure the pulse characteristics, such as rise – fall time and amplitude droop, while in the frequency domain this is impossible. To make accurate measurements, the following relations should be applied [18]:

Pulse width > settling time of analyzer $\cong$ 2/RBW

Rise time of pulse >> rise time of analyzer $\cong$ 0.7/RBW.

In the report of Agilent Radar Measurements application notes [18] in addition to the above three traditional ways Radar measurement that were presented, three other built-in functions and features that can support spectrum analyzers used today are analyzed, and thus simplify and enrich Radar measurements. These are: Channel Power, Occupied Bandwidth, Burst power.

Channel Power

With Channel Power function we can measure the average power across the frequency band of interest. It is a common method of signal measurements and it is often used to measure many different kinds of signals. Modern spectrum analyzers include special software to calculate the power at a given frequency channel. This software calculates the power by integrating the power represented by the displayed trace pixels within the frequency range of the channel bandwidth (IBW = Integrated Bandwidth). For the measurement, the averaging detector is used. The displayed result comes from the computation [29]:

$$P_{Ch} = \frac{B_S}{B_n}\frac{1}{N}\sum_{i=1}^{N} 10^{\frac{Pi}{10}}$$

where:

Pch is the power in the channel.

Bs is the specified bandwidth (also known as the channel bandwidth).

Bn is the equivalent noise bandwidth of the *RBW* used.

N is the number of data points in the summation.

pi is the sample of the power in measurement cell *i* in dB units (if *pi* is in dBm, *Pch* is in milliwatts).

The Resolution bandwidth for the Channel Power measurement should be small compared to the channel bandwidth. If the Resolution bandwidth is too large, the selectivity of the simulated channel filter is insufficient and part of the main channel power will be measured when measuring the adjacent channels, so the final result will be incorrect. Thus, a good value for the RBW can be 1% to 3% of the channel bandwidth. The video bandwidth must be at least three times the resolution bandwidth to avoid averaging of the video voltage [30].

The Channel Power function is very useful when we measure pulsed radar because it has complex signals and often the PRF and the pulse width is changed. Thus, the spectrum of these signals is also complex and the power cannot be easily calculated from the spectrum [31].

Occupied bandwidth (OBW)

Another built in function having spectrum analyzers is the automatic measurement of occupied bandwidth. Occupied bandwidth of the signal is the bandwidth containing 99.0% of the signal's total power. To make the measurement of OBW we set the following settings in the spectrum analyzer [32]:

Span: 1.5 to 2 times the estimated bandwidth of the emission
Resolution bandwidth (RBW): less than 3% of the span
Video bandwidth (VBW): 3 times RBW or more
Detector: peak or sample
Trace: MaxHold
Channel Bandwidth: the highest value of bandwidth of the analyzer.

Burst power

The burst-power measurement is an automated zero-span measurement. In channel power process, we can measure the power in the frequency domain. In burst-power measurement we can have the measurement of power at a specified time slot or gate. The calculation often uses a burst-power trigger. This measurement is very useful for the radar, because it is a direct measurement of the pulse power. The settings at the analyzer are the same as those of Zero span and the RBW should be sufficiently wide.

4.5.1 Radar Measurements according to Narda – sts.

In the report of Narda Radar Measurements application notes [33] the way Radar emission existence can be detected, when the central transmission frequency is not known, is analyzed. It is also explained how measurements in the time domain and in the frequency domain with SAs can be performed. Also, it presents the steps of preparation that are needed before a measurement and the evaluation of the results of measurement with the creation of the corresponding report after the measurement.

The preparation before the measurement includes the collection of information about the operation and the installation of Radar. It is important that the suitable position of measurement shall be determined. Also, a lot of time is needed in order to the collected measurements to be correct.

The measuring equipment has to contain the appropriate devices.

- A spectrum analyzer (if narrowband measurements are performed).
- A portable pc (laptop) with spare batteries (if AC power is not available on site), for controlling the SA, storing measured values, and recording comments.
- A tripod
- RF cable
- A Single-axis E-Field antenna

During the measurement process the antenna has to be as far as possible from any metal parts of tripod or other metal object and the person making the measurement has to be some meters away from the antenna.

Before the measurement is started, an overview measurement in spectrum mode has to be made, covering the frequency range (full span) of the SA. In this measurement the radar frequencies and other transmission sources can be identified. In this case the Resolution Bandwidth has to be wide enough and the trace Mode has to be Max.

If the Radar frequencies are unknown, they can be determined by using the SA. In this case, the frequency range that the SA scans, must be very short and around the Radar frequencies (that probably have been determined during the overview measurement), the Resolution Bandwidth has to be narrow and the Trace Mode has to be Max.

Also, [33] describes the spectrum mode method of measuring Radar, which is the traditional method for measuring electromagnetic waves. In this method we need a large amount of time. This is due to the way that a spectrum analyzer works. On the other hand, the peak value of the measurement can be determined by applying correction factors.

The settings of the SA are:

- **Center frequency**
  The Radar frequency that we know or is determined at the overview measurement. One radar channel must be selected for measurement of dual channel radar.

- **Trace Mode**
  Max
- **Detector**
  Peak
- **Frequency range - Span**
  The frequency span should be selected to be a multiple of the inverse of the pulse width. For example: Pulse width PW = 1μs, Span = 20 x 1/1μs = 20MHz.
- **Resolution bandwidth RBW**
  The resolution bandwidth RBW value should be according the formula:

  $$2\ PRF \leq RBW \ll 1/PW$$

  Example: Pulse repetition frequency PRF = 1kHz, RBW = 2kHz or slightly more.
- **Units: logarithmic**, i.e. dBμV/m, dBmV/m, dBV/m or dBA/m so that correction factors can be applied easily after the measurement

The result of the above method is to find the highest peak and to read the numerical value. This maximum value needs to be corrected by an amount which is dependent on the resolution bandwidth RBW and the pulse width PW.

Separate measurements have to be taken in the three orthogonal spatial axes x, y, and z. The maximum total field strength is calculated by the root sum of the squares (RSS) of the three calculated E – field components according to the following equation:

$$|E_{total}| = \sqrt{|E_X|^2 + |E_Y|^2 + |E_Z|^2}$$

At the end, [33] mentions that the evaluation of the measurements has to include an assessment of the results with reference to the limit values. This is the interesting point for each one. For the evaluation of the measurements the uncertainty of the measurement has to be taken into consideration as well. The measurement report should include the evaluation and the assessment of the measurements. Also, the measurement data and the corresponding graphics should be contained in the measurement report.

4.5.2 Theoretical Calculations for Radar signals

The British Defense Standard [20] describes the theoretical computations for Radar signals. According to it, in the far field the average power density P_T in the axis of maximum gain of the antenna of rotating Radar is given by:

$$P_T = \frac{P_{av} \cdot G}{4\pi d^2} \cdot \frac{\beta}{360}$$

where P_{av} is the average radiated power, G is the antenna gain, β is the half power angle in degrees in the horizontal plane. Due to the ground reflections 6 dB must be added to the result of equation 6.

4.5.3 Measurements of an Air-Traffic Surveillance Radar

In [26] an automatic system that can acquire, store and analyze the electromagnetic radiation emitted from an Air-Traffic Surveillance Radar is described. Also, in this work the operating characteristics of the Radar are verified.

The automatic system carries out measurements of radiation emission from air-traffic surveillance Radars with SA. The Radar measurements can be collected, stored and evaluated and in the end, an automatic report is created. The system can make measurements for both the PSR approach Radar of civil aviation of Greece and the Secondary Radar (SSR).

In work [26], the following operating characteristics of Radar were directly or indirectly measured:

- Rotation period
- Pulse Repetition Frequency
- Pulse width
- Mean received power

The rotation period Δ_t is found by using the follow equation:

$$\Delta t = \frac{\Delta f}{SPAN} \cdot SWP$$

where Δ_f is the frequency difference between two successive peaks, and SPAN is the respective frequency range setting of the SA, SWP is the sweep time which must be used in the spectrum analyzer. SWP must contain at least two peaks during each sweep to measure the rotation period of the radar. During this measure the pulse-spectrum mode of SA was used.

The Pulse Repetition Frequency (PRF) of Radar was measured with the SA at the pulse-spectrum mode. The values of SPAN and the SWP of SA were small in order to be displayed in the SA single pulses rather than pulse trains. Also, the SA must be operated in MAX HOLD. From the equation:

$$\Delta t = \frac{\Delta f}{SPAN} \cdot SWP$$

Δ_t can be calculated and PRF = $1/\Delta_t$

The measurement of Pulse Width was the most difficult task in this work. Because in real emissions of Radar signals, the nulls of the main lobe at the power spectrum are not always observable. According to Fourier analysis, the main lobe of a pulse spectrum has a half-width of $\Delta_f = 2/\tau_{eff}$ from which the effective pulse width can he calculated. The way which was proposed was to use the distance between the first sidelobes, which is $\Delta_f=3/\tau_{eff}$. The SA settings had a large enough SPAN, a small SWT and MAX HOLD operation.

The calculation of the average radiated power from the Radar, P_{av}, can be made from the equation $P_{av} = P_{peak} * \tau_{eff} * PRF$. The peak value, P_{peak}, and the duty cycle = τ_{eff}*PRF were also measured (where τ_{eff} , is the effective pulse width).

Chapter 5 – Uncertainty of Measurement

5.1 General Remarks

The uncertainty of measurement is the difference between the actual value of a quantity which is measured and the final result of a measurement process [34]. Thus, the uncertainty of measurement is a very important element in the accurate calculation of the actual value of the measured quantity. For this reason, it should be properly determined. Two of the most important publications in the area of Electromagnetic Compatibility (EMC) and Measurement Uncertainty (MU) are LAB 34 [35] and CISPR 16-4-2. EMC. LAB 34 is published by the United Kingdom Accreditation Service (UKAS). CISPR 16-4-2 is published by the International Electrotechnical Commission (IEC). Both Measurement Uncertainty documents are based on the International Standards Organization (ISO) Guide to the Expression of Uncertainty in Measurement (GUM) [36], 1993, corrected and reprinted in 1995.

Initially, in order to assess the uncertainty of the measurement of a quantity is to find all factors that introduce an error in measurement, whether they are external in relation to the measuring system or internal. Errors in measurement are created from random effects and systemic effects. Random effects caused by random events and their values change if the measurement is repeated under exactly the same conditions. They cannot be eliminated, but increasing the number of observations and applying statistical analysis may reduce the uncertainty due to their effect. The systemic effects are inherent in the equipment which is used in measurement (instruments, cables, etc.) and in the measurement method. Their value will not change if the measurement is repeated under exactly the same conditions. They cannot be eliminated but may be reduced.

According to [35], [37] the uncertainties are divided into two categories based on the calculation of the components. These are: ‘Type A’, which are calculated using statistical methods. ‘Type B’, which are calculated in different ways to those used for ‘Type A’, for example, from the manufacturer's specifications (datasheets) or from measurements from previous experience or from data in calibration certificates.

For the calculation of the overall measurement uncertainty the next steps are followed:

We describe each uncertainty component which contributes to the overall uncertainty with a calculated standard deviation and is referred to as a Standard uncertainty (standard uncertainty – u(xi)).

We calculate the combined standard uncertainty u_c. On the condition that the components are stochastic and independent of each other and affect the total uncertainty cumulatively. Thus, the combined standard uncertainty is obtained by taking the square root of the sum of the squares of standard uncertainties (RSS).

We estimate the expanded uncertainty by multiplying the combined standard uncertainty by a constant k which is called coverage factor. For example, when the combined standard uncertainty follows normal distribution the expanded uncertainty corresponds to a confidence level 68%, with k = 1, and corresponds to a confidence interval of 95%, with k = 1,96. (If k =1,96, then the overall uncertainty will lie in the range $2 \times u_c$ with probability 95%).

Usually the information for the uncertainty factors (for example, from manufacturer in the datasheets) is given in the form ± a, so, the upper (+ a) and lower (-a) limit of the uncertainty or the space where the uncertainty lies (2a) are given. The values of the uncertainty can be at the form of percentage (%) or at the form of db. When uncertainty components are not expressed in the same units (% rate or dB), before calculating the combined standard uncertainty, all of the expressions in the same unit must be converted. The % rate is selected as a common unit. It is more correct to express the uncertainty of measurement in percentage (%) than in db because in this way the smaller error occurs in the calculation [38] [39].

In order to determine the standard uncertainty of each contribution it should be associated with a probability distribution. The probability distribution of the measured quantity describes the variation in probability of the true value lying at any particular difference from the measured or assigned result. The four main distributions which are used in EMC measurements are normal, rectangular, triangular, and U shaped [35].

Normal:

This distribution can be assigned to uncertainties derived from multiple contributions. The standard uncertainty of a contribution with this distribution is found by dividing the expanded uncertainty by the coverage factor, k = 2, with 95% level of confidence. So,

$$u(xi) = \frac{expanded\ uncertainty}{2}$$

Rectangular:

Rectangular distribution means that there is equal probability of the true value lying anywhere between two prescribed limits. If the manufacturer does not give any data on the distribution of uncertainty, we assume that a rectangular distribution is followed and thus the standard uncertainty will be equal to:

$$u(xi) = \frac{a_i}{\sqrt{3}}$$

where a_i is half the length of the interval given by the prescribed limits of the individual uncertainty contribution.

U Shaped:

U shaped distribution is applicable to mismatch uncertainty (M). M is associated with the power transfer at a junction and its value is given by the following equation if the source and the load are straightly connected. M is associated with the power transfer at a junction between two devices and its value is given by the following equation if both devices are directly connected [37].

$M = |\Gamma_A||\Gamma_B| * 100\%$

Where $|\Gamma_A|$, $|\Gamma_B|$ are the reflection coefficients for the two devices.

It is applied that: $|\Gamma| = \frac{VSWR-1}{VSWR+1}$, where VSWR is the voltage standing wave ratios of the devices.

The standard uncertainty for the mismatch will be equal to:

$$u(xi) = \frac{M}{\sqrt{2}}$$

Triangular:

Triangular distribution means the probability of the true value lying at a point between two prescribed limits increases uniformly from zero at the extremities to the maximum at the center. If two identical rectangular distributions, each of magnitude ± a, are combined, then the resulting distribution will be triangular with a semi-range of ± 2a. For this distribution the standard uncertainty will be equal to:

$$u(xi) = \frac{a_i}{\sqrt{6}}$$

where a_i is half the length of the interval given by the prescribed limits of the individual uncertainty contribution.

Determination of the combined standard uncertainty:

In order to determine the combined standard uncertainty u_c, if any of the standard uncertainties are not already expressed in the measured quantity, then they should be converted by using the appropriate sensitivity coefficient c_i, and then: $u_i = c_i u(xi)$. The sensitivity coefficient c_i is effectively a conversion factor from one unit to another because in some cases an input quantity may not be in the same units as the associated output quantity. When all the quantities influencing the uncertainty of measurement are uncorrelated (this is usually the case in EMF measurements), then all the sensitivity coefficients will be $c_i = 1$ [40]. Then the combined standard uncertainty u_c will be equal to:

$$\boldsymbol{u_c = \sqrt{\sum_{i=1}^{N} u_i^2}}$$

5.2 Calculation of uncertainty of measurement system for electromagnetic radiation from Radar

The calculation of the uncertainty of measurement for electromagnetic radiation from Radar for the used measurement system, was carried out according to [40] [41] [42]. The quantities that contribute to the uncertainty of measurement for the radar system are uncertainties of type 'B'. The repeatability uncertainty (which is type 'A') is equal to zero, because for the calculation of power density and electric field strength we use the maximum measurement value of the spectrum analyzer.

In this work, we used a single-axis E-field dipole antenna. In order to achieve the simulation of isotropic reception of the fields, we carried out measurements in the three polarizations X, Y, Z. So, the combined standard uncertainty $u_{c(Epi)}$ for each polarization has to be calculated separately and then the total combined standard uncertainty $u(E_c)$ will be calculated [42]. So, we have:

$$u(E_c) = \sqrt{\sum_{Pi=1}^{3} u_{(Epi)}^2}$$

In this work, the combined standard uncertainty in each polarization is the same because the antenna factor has the same value at each polarization according to the calibration certificates (CCs) and the manufacturer specification data sheets (SDSs) do not give information on the display scale fidelity uncertainty. Moreover, we carried out measurements at one frequency and not at a band of frequencies.

Figure 5.1 shows the measurement system that was used in this work. All the devices and the connections that can contribute to the uncertainty of measurement are illustrated.

Figure 5.1 The Measurement system

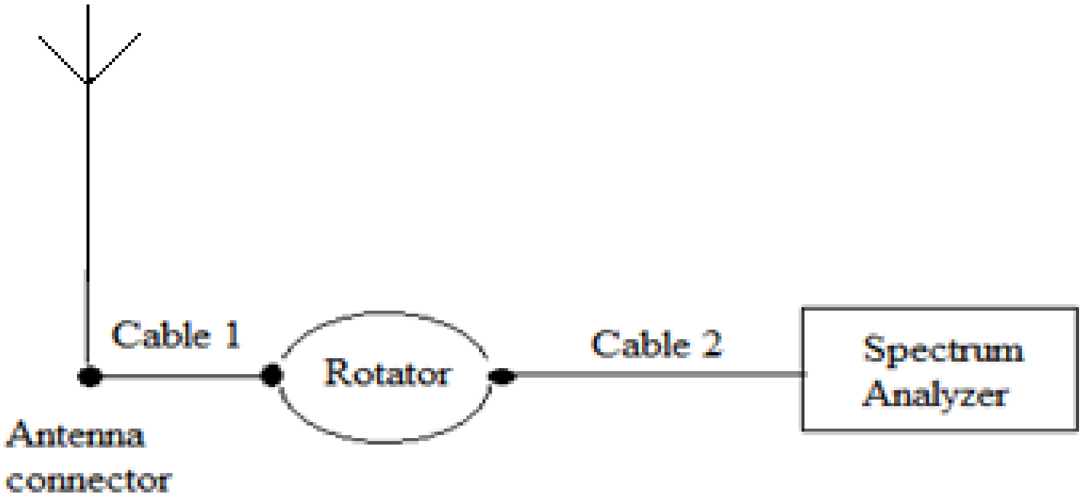

Table 5.1 shows the quantities that contribute to the uncertainty of measurement for the radar system for each polarization and their values of standard uncertainty u(xi) in percentage (%).

Table 5.1 Elements of Uncertainty for each polarization

The combined standard uncertainty u_c in each polarization will be equal to:

A/A	PARTIAL UNCERTAINTIES	Type	Value	Probability distribution	Divisor	C_i	*u(xi)* %
1	**Repeatability uncertainty**	A	0				0
	Spectrum Analyzer						
1	Sweep	B	3%	---	K=√3	1	1.5
2	Span	B	1%	---	K=√3	1	0.5
3	Reference Calibration	B	0 dB	Normal	K=2	1	0
4	Resolution BW	B	5%	---	K=√3	1	2.5
5	Frequency response	B	0.95 dB	----	K=√3	1	6.6
6	Refer level	B	0.1 dB	----	K=√3	1	0.66
7	Attenuator uncertainty	B	0.254 dB	----	K=√3	1	1.7
8	Total measurement uncertainty	B	1dB	----	K=√3	1	7
	Mismatch	B					
1	Antenna - Rotator	B	3.63 %	U Shaped	K=√2	1	2.57
2	Rotator - SA	B	3.63 %	U Shaped	K=√2	1	2.57
	Antenna						
1	Antenna Factor	B	1,8 dB/2=0.09dB	Normal	K=2	1	1.04
	Cables						
1	RG400	B	-0.04…0.04 dB/2=0.02dB	Normal	K=2	1	0.23
2	RG178	B	-0.04…0.04 dB/2=0.02dB	Normal	K=2	1	0.23
	Combined standard uncertainty in each polarization			Normal			$u_{c(Epi)}$ =9.46 %
	Desired coverage probability p						**95%**
	Corresponding coverage factor of k						**1.96**

$$u(E_{pi}) = \sqrt{\sum_{i=1}^{N} u^2{}_{(xi)}} =$$

$$\sqrt{0^2 + 1.5^2 + 0.5^2 + 0^2 + 2.5^2 + 6.6^2 + 0.66^2 + 1.7^2 + 2.57^2 + 2.57^2 + 1.04^2 + 0.23^2 + 0.23^2} = \\ = 10.9\%$$

The total combined standard uncertainty $u(E_c)$ for the three polarization of antenna will be equal to:

$$u(E_c) = \frac{1}{E_{B,P}} \sqrt{\sum_{Pi=1}^{3} E_{B,P,i}^2 u_{(E,P,i)}^2}$$

Where: $E_{B,P}$ is the total electric field strength for the three polarizations.

$E_{B,P,i}$ is the electric field strength for the each polarization.

Desired coverage probability p = 95 %
Corresponding coverage factor of k = 1.96

So, the expanded uncertainty $U(_E)$ with a 95% coverage probability coverage factor k=1.96 (normal distribution) will be equal to:

$U(_E) = k\ u(E_c)$

According to [42] the associated combined standard and expanded uncertainties for E, H, B, and S will be given by

$u(E) = u(H) = u(B) = \frac{u(S)}{2}$.

So, U(S) = U(E) * 2

<u>The following formulas are applied:</u>

The conversion of dB to percentage (%) can be made with the following formula:

$\frac{(100*(|(1-10^{\frac{db}{20}})|)}{divisor}$, the result is the standard uncertainty in percentage (%).

$|\Gamma| = \frac{VSWR-1}{VSWR+1}$, the reflection coefficient of a device.

VSWR (SA) = 2dB

VSWR (rotator) = 1.25 dB

Mismatch = $\frac{|\Gamma_a|*|\Gamma_b|}{\sqrt{2}} 100\%$, the result is the standard uncertainty of mismatch in percentage (%).

Chapter 6 – Detailed description of measurement

In this work, measurements for the estimation of the electromagnetic burden of Radar were carried out by using an automatic system.

So, in this work measurements for the estimation of the electromagnetic burden of the Surveillance Radar (PSR) of Nikos Kazantzakis airport of Heraklion, Crete were made for testing purposes. The Primary Surveillance Radar of the Nikos Kazantzakis airport is located in Dyo Aorakia area in the Municipality of Heraklion. Geographical position: 35 19'39.50'' N 25 10' 21.36''E. It belongs to the Hellenic Civil Aviation Authority. The appropriate equipment of the Non Ionizing Radiation Laboratory (NIRL) of Technological Educational Institute of Crete was used. All devices are accompanied by certificates of quality, calibration and excellent operation. The measurements were carried out with spectrum analyzer (Narrowband measurements). The place which was chosen for the measurements is close to TEI of Heraklion and it is in line of sight with the Radar. Geographical position: 35 19'41.80'' N 25 09' 51.98''E. For this purpose, two dedicated software applications were developed in MATLAB environment one for the remote control of the used instrumentation and the collection of the measurement data and the other for the processing of them. The great benefit of this manner of measurement is that random errors caused by the personnel employed in the measurement procedure are avoided. The remote communication with the measurement system and the post processing of the measurement data is done by using two Graphical User Interfaces (GUI) developed in MATLAB.

Two types of Radars are used in air traffic control, the primary and the secondary Radar. The secondary Radar is an interrogator. It transmits a question and the aircraft responds by its transponder and gives information such as its identity and height. Since the secondary Radar does not receive its own transmitting signal, it operates at a much lower power level than the primary Radar. For this reason, measurements concerning the human safety are not necessary for the secondary Radar [33]. So, in this work measurements for the secondary Radar of Nikos Kazantzakis airport of Heraklion were not carried out.

In previous chapters, the appropriate algorithm and the settings that were used for the procedure of measurement were described. In this section, all the values of the settings will be presented in an analytical manner.

Average and peak values of power density and electric field strength at the frequencies of the carrier of the primary radar (2760MHz, 2840MHz) determine the electromagnetic effect of the radar. During the measuring operation, the channel with the operating frequency of 2840 MHz was in working order, so measurements were made only at this frequency.

The duration of a scan (t = 5sec> Trot) should be sufficient to register a pulse. A period of 30 min was chosen as a measurement time at each polarization so that the spectrum of the signal can be correctly formed in the SA. Thereby, the requirements of the ICNIRP directives were covered on average during a six-minute measurement.

The Nikos Kazantzakis RSR Radar technical characteristics were known during the process of measurement and they are presented in Table 6.1.

Table 6.1 Technical features of N. Kazantzakis PSR

Frequency	2840 /2760 MHz
Peak Power	1200 KW
Average Power	1200 W
Pulse duration	1μsec
Pulse repetition period	1msec
Duty Cycle	1/1000 =0.001

The devices used in the measurement and the connections between them are shown in figure 6.2. The detailed description of these devices is:

1) The **Spectrum Analyzer** used for the measurements is Rohde & Schwarz model FSH8, achieving 631 sweep points (Figure 6.1).

2) The **Antenna** used is a single-axis E-field dipole antenna, type: PCD 8250 from Austrian Research Centers – ARC. An omnidirectional antenna is not available at the Non Ionizing Radiation Laboratory of Technological Educational Institute of Crete. So, in order to simulate an isotropic reception of the fields, a subroutine controlling the rotation of the antenna in three mutually perpendicular polarizations named X, Y and Z has been developed in the software for the collection of measurement data. The rotation of the antenna is controlled by this subroutine without the involvement of the operator (Figure 6.1).
3) A **Laptop.** The software of the remote communication with the measurement system and the post processing software of the measurement data are running on a laptop computer, in MS Windows Environment. The laptop is connected to the SA with an Ethernet cable and to the antenna rotator with a USB cable. After the end of measurements, the measurement data for each polarization of the antenna are saved for further processing in an MS Excel file in the laptop.
4) Two **RF – Cables.** Type: RG400 and RG178. The first one is used to connect the antenna to the rotator and the second one is used to connect the rotator to the SA. Also, a USB cable and an Ethernet cable are used.
5) A **Tripod** for the antenna support.

The whole equipment is portable, for easy transportation to the measurement places.

Figure 6.1 Spectrum Analyzer and ARC-PCD8250 Antenna

Figure 6.2 The diagram of the measurement system

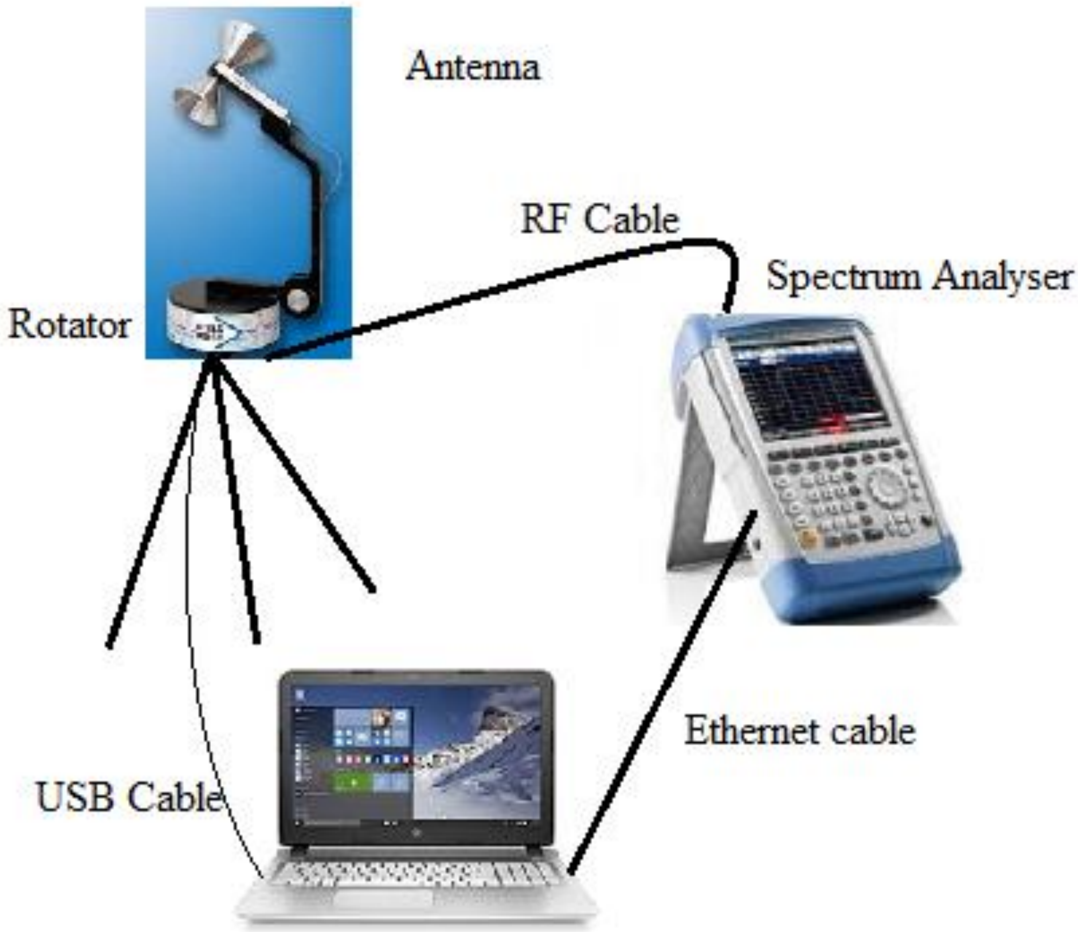

6.1 Configuration of SA during measurements

The necessary settings for the spectrum analyzer have been incorporated in the code of the software for the collection of measurement data and were selected according [33]. Table 6.2 shows these settings.

Table 6.2 Configuration of SA during measurements

Center frequency	2840MHz (or 2760MHz)
Mode of operation	Spectrum Mode
SPAN	20 MHz
Trace Mode	MAX HOLD
Detection Mode	Positive peak
RBW	>PRF=3 KHz
Sweep time	> T_{rot} =5 sec ($T_{rot\ Radar}$=4 sec)
VBW	≥ RBW =3KHz

The obtained spectrum of the Nikos Kazantzakis RSR Radar is shown in Fig. 6.3

It should be noted that in order to record the highest value of the signal for each scan, the trace mode of MAX HOLD was selected. The Positive peak in the Detection mode was selected, so the peak value of the signal was displayed.

Figure 6.3 Power spectrum of Nikos Kazantzakis PSR

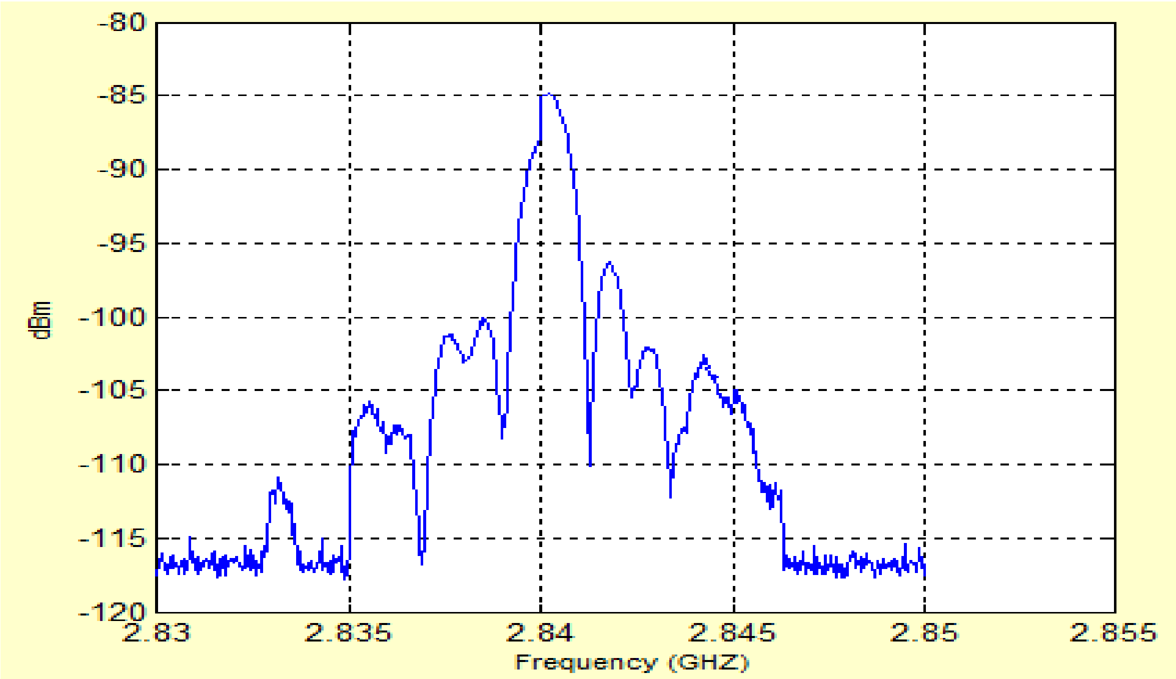

6.2 Calculation of the Electric field strength – E and Power density – S_{eq}

After the end of the measurements the second GUI was used for post processing the measurement data. The final results of the post processing, due to the Radar under examination, are the total Electric field strength E and equivalent plane wave Power density S_{eq} arisen at the place of the receiving antenna. These values are then compared to the maximum permissible exposure values that have been legislated in Greece [43] [44].

From each of the three measurement files for each polarization the maximum value was selected. Each max value was corrected with the total instrumentation losses (cable and connector losses) and the antenna gain value in order to calculate the maximum received power at the place of the receiving antenna. Then, the received power was converted to electric field strength, and the value of the electric field strength was corrected according to the equation $a_p = 20 \log (k^* \tau_{eff} RBW)$ db in order to evaluate the maximum received electric field for each polarization (X,Y and Z) [45].

The maximum total electric field strength is calculated by the root sum of the squares (RSS) of the three calculated E - field components according to the following equation:

$$|E_{total}| = \sqrt{E_X^2 + E_Y^2 + E_Z^2}$$

where E_X, E_Y and E_Z are the three calculated components of the electric field strength at the three antenna polarizations. For human exposure from pulsed emissions, the average of S_{eq} (W/m^2) throughout the pulse width should not exceed 1000 times the respective RLs. Also, the field strength values must not exceed 32 times the RLs for the respective field strength.

The total maximum received electric field strength has to be compared with these limits after taking into account the uncertainty of the measurement system. The average electric field strength can be calculated from the following equation where the Duty Cycle of the Nikos Kazantzakis PSR Radar is 1μsec/1msec=1/1000 [19].

$$E_{peak} = \frac{E_{av}}{\sqrt{duty\ cycle}}$$

The results of the comparison with the limits derived from the post processing GUI are shown in Fig. 6.4. Fig. 6.5 shows the isotropic E field strength graph of the Radar as derived from the post processing GUI.

For pulsed Radar signals, the exposure ratio λ, is given by the following equation and must be <1, so as to characterize the Radar emission as an emission under the exposure limits at the place of measurements:

$$\lambda = \frac{E_{av}^2}{(32*L_E)^2} = \frac{H_{av}^2}{(32*L_H)^2} = \frac{S_{av}}{1000*L_S}$$

where E_{av} is the average value of the electric field strength, H_{av} is the average value of the magnetic field strength, S_{av} is the average value of equivalent plane wave power density, and L_E, L_H and L_S are the corresponding RLs of E_{av}, H_{av} and S_{av}.

Figure 6.4 The results of the comparison with the limits

Lamda Eav/Sav	Uncertainty U(E)(%)	Power Density U(S) Uncertainty (%)
9.95387e-09	21.384	42.768

- Results of Radar Measurments -

	Value	Uncertainty	Total Value	Limit Compare
Epeak (V/m)	3.92578	0.839491	4.76527	316.96
Eav (V/m)	0.124144	0.026547	0.150691	313.223
Speak (W/m^2)	0.0408801	0.0174836	0.0583637	102804
Sav (W/m^2)	4.08801e-05	1.74836e-05	5.83637e-05	102804

Figure 6.5 E field strength isotropic graph

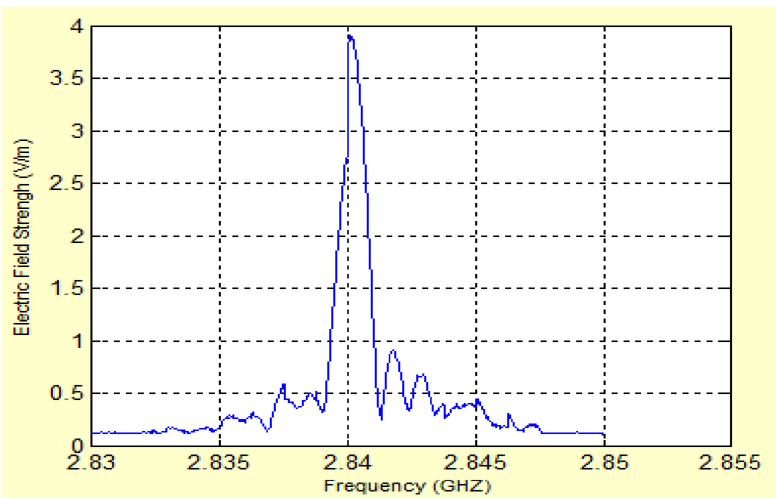

The detailed description for the calculation of the total Electric field strength E and equivalent plane wave Power density S_{eq} arisen at the place of the receiving antenna is:

Measured Values from each of the three measurement files for each polarization.

Xmax= -101,69 dbm

Ymax = -84,95 dbm

Zmax= -84,90 dbm

Calculation of E_{peak} for the X polarization

Xmax= -101,69 dbm

Measurement System Losses:

Connectors = 0.3 db

Both PCD Cables Attenuation (third order splines algorithms were used) = 11.71 dB

Total loss = 12,01 db

Antenna P_{max} = -101,69 + 12,01 = -89.68 dbm

Maximum voltage at the antenna V_{max} : -89.64 +107 = 17,32 dBμV

AF dB/m (fi) = 44.83 dB/m (third order splines algorithms were used).

Maximum Electric Field at the antenna E_{max}:

dBμV + AF (dB/m) = 17,36 + 44.83 = 62,15dBμV/m

Desensitization factor:

$a_p = 20 \log (k^* \tau_{eff}\ RB)$ db = 20log(1.065 10^{-6} 3000) = - 49.91 db

Maximum Electric Field at the antenna is corrected with desensitization factor:

$P_{correct}$ = 62,19 –(-ap) = 62,32 +49.91 = 112,06 dBμV/m

Maximum Electric Field at the antenna in V/M

$$E_{peak} = (10^{\frac{E\frac{db\mu V}{m}}{20}})/1000000 = (10^{\frac{112,06}{20}})/1000000 = 0,40 \text{ V/M}$$

Calculation of E_{peak} for the Y polarization

Ymax= -84,95 dbm

Measurement System Losses:

Connectors = 0.3 db

Both PCD Cables Attenuation (third order splines algorithms were used) = 11.71 dB

Total loss = 12,01 db

Antenna P_{max} = -84,95 + 12,01 = -72,94 dbm

Maximum voltage at the antenna V_{max} : -72,9 +107 = 34,06 dBμV

AF dB/m (fi) = 44.83 dB/m (third order splines algorithms were used).

Maximum Electric Field at the antenna E_{max}:

dBμV + AF (dB/m) = 34,1 + 44.83 = 78.89 dBμV/m

Desensitization factor:

$a_p = 20 \log (k^* \tau_{eff} RB)$ db = $20\log(1.065\ 10^{-6}\ 3000)$ = - 49.91 db

Maximum Electric Field at the antenna is corrected with desensitization factor:

$P_{correct}$ = 78.93 –(-ap) = 78.93 +49.91 = 128,8 dBμV/m

Maximum Electric Field at the antenna in V/M

$E_{peak} = (10^{\frac{E\frac{db\mu V}{m}}{20}})/1000000 = (10^{\frac{128,8}{20}})/1000000$ =2,75 V/M

Calculation of E_{peak} for the Z polarization

Zmax= -84,90 dbm

Measurement System Losses:

Connectors = 0.3 dB

Both PCD Cables Attenuation (third order splines algorithms were used) = 11.71 dB

Total loss = 12,01 dB

Antenna P_{max} = -84,90 + 12,05 = -72,89 dBm

Maximum voltage at the antenna V_{max} : -72,85 +107 = 34,11 dBμV

AF dB/m (fi) = 44.83 dB/m (third order splines algorithms were used)

Maximum Electric Field at the antenna E_{max}:

dBμV + AF (dB/m) = 34,15 + 44.83 = 78.94 dBμV/m

Desensitization factor:

$a_p = 20 \log (k^* \tau_{eff} RB)$ db = $20\log(1.065\ 10^{-6}\ 3000)$ = - 49.91 db

Maximum Electric Field at the antenna is corrected with desensitization factor:

$P_{correct}$ = 79,11 –(-ap) = 78.98 +49,91 = 128.85 dBμV/m

Maximum Electric Field at the antenna in V/M

$E_{peak} = (10^{\frac{E\frac{db\mu V}{m}}{20}})/1000000 = (10^{\frac{128{,}85}{20}})/1000000$ =2,77 V/M

So, the **maximum peak value of the total field strength** is:

$E_{\text{total peak}} = \sqrt{Exmax^2 + Eymax^2 + Ezmax^2} = \sqrt{0{,}4^{\,2} + 2{,}75^2 + 2{,}77^{\,2}} =$
$\sqrt{0{,}161 + 7{,}72 + 7{,}72}$ = 3.92 V/m

The uncertainty of the measurement system.

In the previous chapter the combined standard uncertainty u_c in each polarization was calculated and we have:

The combined standard uncertainty u_c in each polarization:

$u(E_{pi}) = \sqrt{\sum_{i=1}^{N} u^2{}_{(xi)}} =$

$\sqrt{0^2 + 1.5^2 + 0.5^2 + 0^2 + 2.5^2 + 6.6^2 + 0.66^2 + 1.7^2 + 2.57^2 + 2.57^2 + 1.04^2 + 0.23^2 + 0.23^2} =$
$= 10.9\%$

The total combined standard uncertainty $u(E_c)$ for the three polarizations of the antenna will be equal to:

$$u(E_c) = \frac{1}{E_{B,P}} \sqrt{\sum_{Pi=1}^{3} E_{B,P,i}^2 u_{(E,P,i)}^2}$$

Where: $E_{B,P}$ is the total electric field strength for the three polarizations = 3.94 V/m

$E_{B,P,i}$ is the electric field strength for each polarization.

$E_{B,P,x}$ = 0.40 V/m

$E_{B,P,y}$ = 2.75 V/m

$E_{B,P,z}$ = 2.77 V/m

$u(E_c) = \frac{1}{3.94}\sqrt{0.402^2 * 10.9^2 + 2{,}78^2 * 10.9^2 + 2{,}78^2 * 10.9^2}$=10.92 %

Desired coverage probability p = 95 %
Corresponding coverage factor of k = 1.96

So, the expanded uncertainty $U_{(E)}$ with a 95% coverage probability the coverage factor k = 1.96 (normal distribution) will be equal to:

$U(_E) = k*u(E_c) = 1.96*10.92\% = 21.38\%$
According to [42] the associated combined standard and expanded uncertainties for E, H, B, and S is given by

$u(E) = u(H) = u(B) = \frac{u(S)}{2}$.

So, U(S) = U(E) * 2 =21.38%*2= 42.76%

E-field strength E

Expanded uncertainty $U(_E)$ = **21.38%**

So, Epeak = 3.92 V/m with the uncertainty $U(_E)$ = **21.38%** :

3.92*21.38/100=0,83 V/m.

Epeak = 3.92+0,83 = 4,75 V/m (Peak value)

National limit for the E-field strength = 47.2 V/m

Epeak : (32*47.2)/4,75 = 316.96 times below the corresponding limit.

$$Eav = Epeak*\sqrt{dutycicle} = 3.92\sqrt{\frac{1}{1000}} = 0{,}12\ V/m$$

Expanded uncertainty $U(_E)$ = **21.38%**

So, Eav = 0,12 V/m with the uncertainty $U(_E)$ = **21.38%** :

0.12*21.38/100=0,03 V/m.

Eav = 0,12+0,03 = 0,15 V/m

Eav: 47,2/0,15= 313.2 times below the corresponding limit.

For pulsed Radar signals, the exposure ratio λ, is given by the following equation and must be <1, so as to characterize the Radar emission as an emission below the exposure limits at the place of measurements:

$$\lambda = \frac{E_{av}^2}{(32*L_E)^2} = \frac{H_{av}^2}{(32*L_H)^2} = \frac{S_{av}}{1000*L_S}$$

where E_{av} is the average value of the electric field strength, H_{av} is the average value of the magnetic field strength, S_{av} is the average value of equivalent plane wave power density, and L_E, L_H and L_S are the corresponding RLs of E_{av}, H_{av} and S_{av}.

So, $\lambda = \frac{E_{av}^2}{(32*L_E)^2} = \frac{0.14^2}{(32*47.2)^2} = 9{,}95 * 10^{-9} < 1$

Thus, the received Radar signal at the location where the measurements took place is below the limits.

<u>Equivalent plane wave power density S</u>

$S_{peak} = E_{peak}^2$ / 377 = 3.92^2/377 = 0,041 W/m^2

The Expanded uncertainty U(S) is: U(S) = 42.76%

So, S_{peak} = 0,041 W/m^2 with the uncertainty $U_{(S)}$ = **42.76%** :
0.041*42.76/100=0,017 W/m^2.
S_{peak} = 0,041 + 0, 017 W/m^2
S_{peak} = 0,041 + 0,017 = 0,058 W/m^2

National limit for the Equivalent plane wave power density S_{eq} = 6 W/m^2
S peak : 6000/0,058 = 102804 times below the corresponding limit

$S_{av} = E_{av}^2$ / 377 = $0{,}12^2$/377 = $4.08*10^{-5}$ W/m^2 average

So, S_{av} = $4.08*10^{-5}$ W/m^2 with the uncertainty $U_{(S)}$ = **42.76%** :
$4.08*10^{-5}$ *42.76/100=$1.74*10^{-5}$ W/m^2

S_{av} = $4.08*10^{-5}$ + $1{,}74*10^{-5}$ = $5.83*10^{-5}$ W/m^2

S_{av} : $6/5.83*10^{-5}$ = 102804 times below the corresponding limit.

6.3 The Measurement point and photos

The place, where the measurements of Radar took place and some photos from this process are displayed below.

Figure 6.6 Measurement point and Photos from the process of measurement


HKK-1013

Chapter 7 - Software application for radar measurements

7.1 Collection of the measurement data

The measurement GUI is opened via the processing GUI. The application starts with the GUI that controls the SA to perform the Radar measurements. First of all, the communication of the PC with the SA has to be established. Assuming that the SA supports an Ethernet connection (R&S FSH8 supports it), it is obtained using one of the available choices which are: “Direct connection to the analyzer” or “Manually give the analyzer IP”. With the choice “Direct connection to the analyzer” the analyzer must have a constant IP address which has been a priori set to the software (169.254.26.200 has been chosen for the described software).

The second step is to define the folder in which the files containing the measurement data will be stored. These files are stored in MS Excel format and the default path is “C:\Report Temp” followed by the desired name of subfolder.

The third step is to select the cables that are used for the measurement and of course the used antenna. In our case the used antenna was the dipole type PCD8250 antenna from ARC, which is rotated in three mutually perpendicular polarizations by the ARC antenna rotator, in order to simulate isotropic characteristics (isotropic antenna is not available in our laboratory for the frequencies of the Radar signal under examination). For the rotation, the software has to establish communication with the antenna rotator, if such an instrument is used for the measurements. In our case, the ARC antenna rotator is controlled by an Arduino chip (the original rotator manufacturer chip has been replaced in our laboratories). The connection between the rotator and the PC is established via USB cable, and because of the Arduino existence the rotator is recognized as a serial port by the PC. This means that the necessary USB to serial drivers have to be installed firstly on the PC. The software gives two options for this connection. In the “Manually mode” the user of the software has to introduce the correct rotator COM port name, and in the “Auto mode” the software finds it automatically searching all the available PC COM ports and examining the answer to a set of commands from PC to the serial port asking for the existence of the rotator. Also, the software gives the user the option to select the desired antenna polarization(s) for the measurements. If no rotator is used, the “None” shall be selected and if isotropic measurements have to be simulated from dipole like antennas from three measurements (as in our case) the choice “all X and Y and Z” has to be selected.

The choice “Edit Auto Settings for Radar measurement” is used if the user wants to change any default setting of the SA (e.g., RBW, VBW, Sweep time etc.) predefined for the measuring the Radar signals. The last step is to choose the center frequency of the Radar signal (either “RADAR with center frequency 2840 MHz” or “RADAR with center frequency 2760 MHz”). The measurements begin pressing the button “Perform the Selected Measurements”.

Information about the progress of the measurements is displayed in the “Information during measurements” window. The necessary settings for the spectrum analyzer have been incorporated in the code of the software (Table 6.2).

At the end, information about cable attenuation, calibration data and antenna’s antenna factor can be displayed when the appropriate menu button is pressed.

The software developed for the collection of the measurement data uses SCPI commands [46] for communication between PC and SA.

Also, in the PC, Virtual Instrument Software Architecture (VISA) library for SCPI translation of two-way communication between the computer and the SA has to be installed. The developed software uses TCP/IP protocol for communication.

In Fig. 7.1 and Fig. 7.2 screenshots of the GUI used for performing the measurements and the respective simplified flow chart are presented.

Figure 7.1 The GUI for performing civil aviation Radar measurements

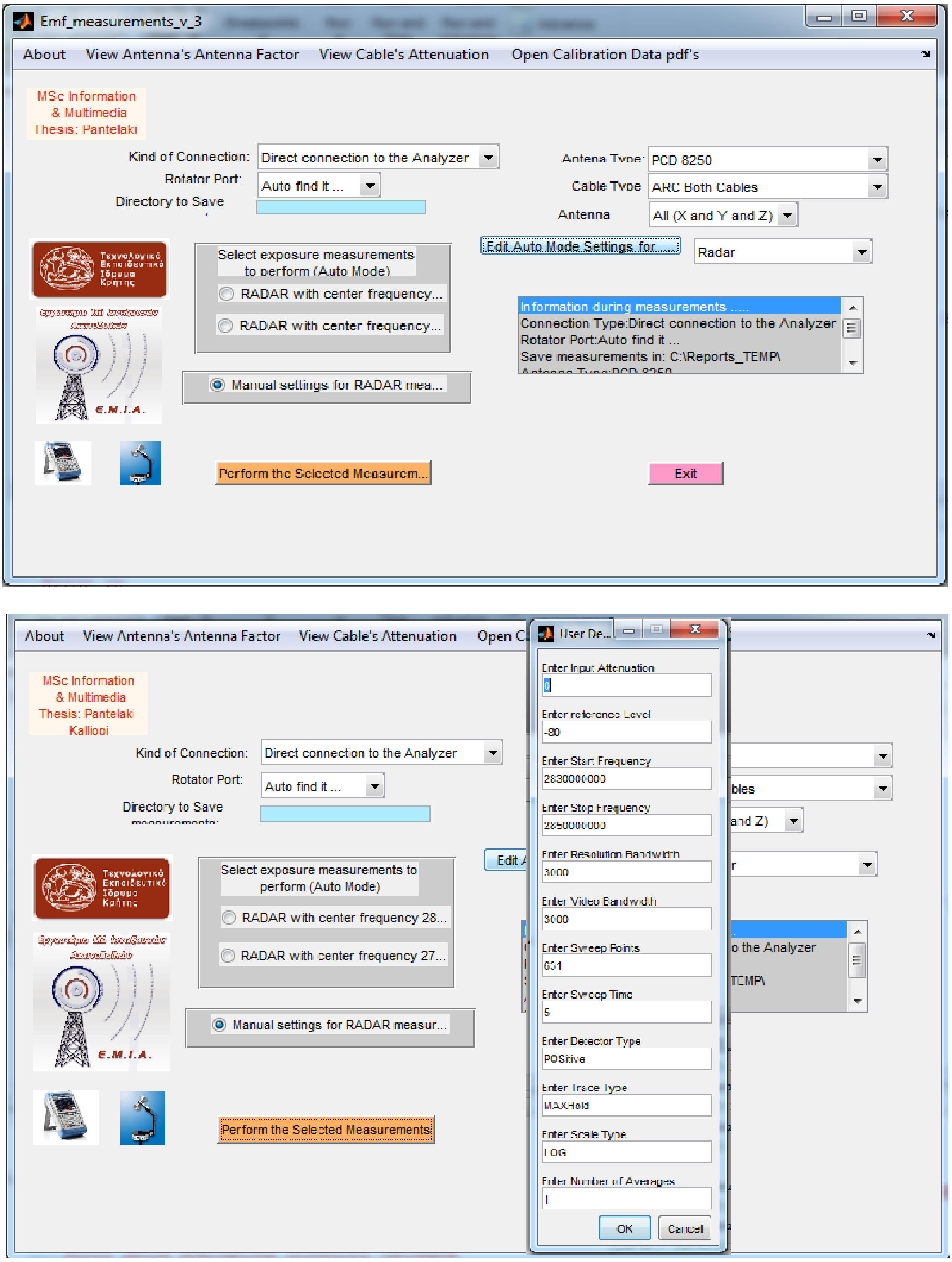

Figure 7.2 Simplified algorithm for GUI for performing civil aviation Radar measurements

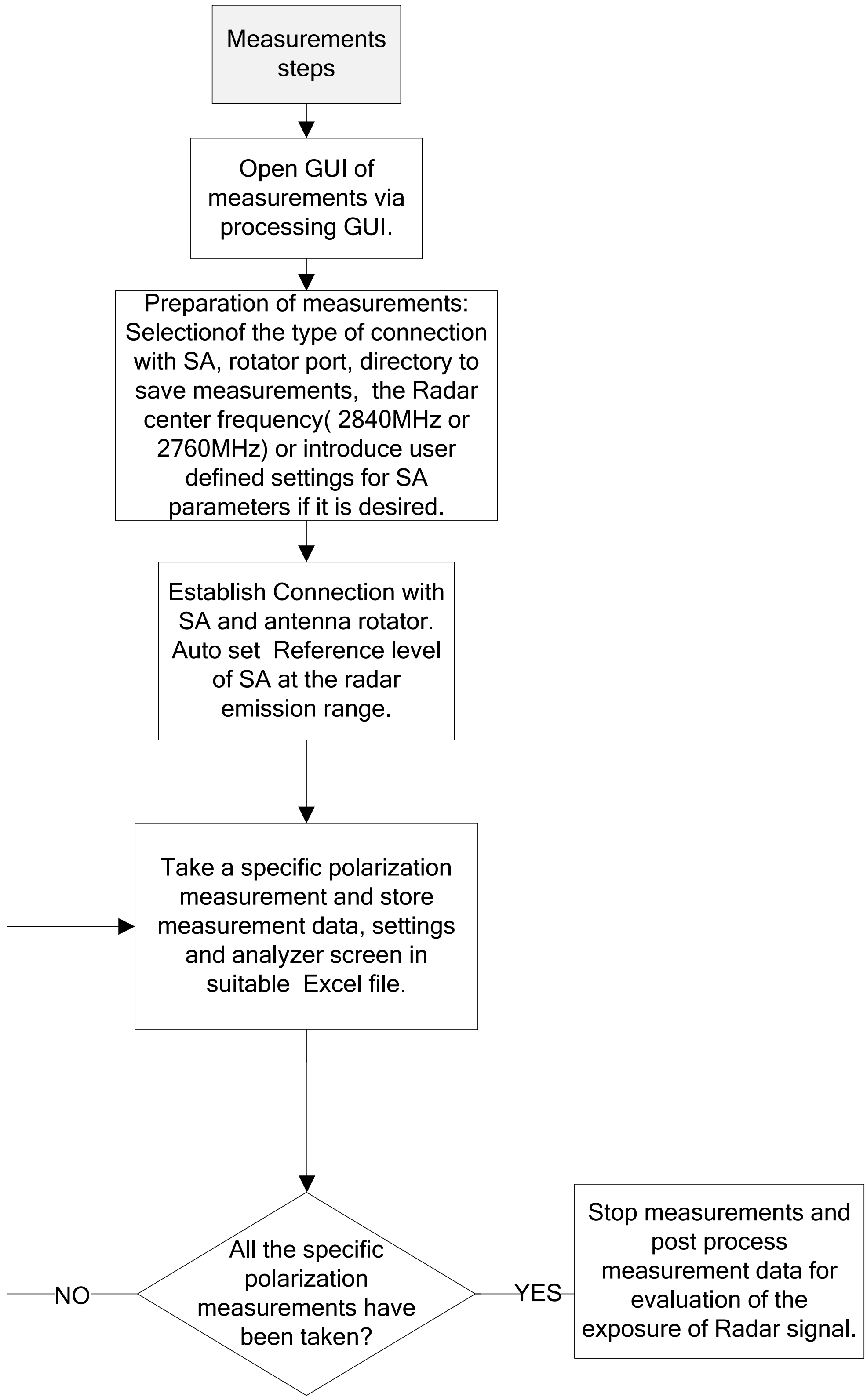

7.2 Post processing of the measurement data

When the desired measurements have been concluded, a second GUI supports the post processing of the collected data (Fig. 7.3). For our case, since we use three polarizations of the received antenna, three MS Excel type files with measurement data have been stored in a user defined directory under "C\ReportsTemp". For the post processing, these files are initially loaded and the available measurement and settings data fill the proper tables of the software.

Pressing the "E isotropic" button, the isotropic graph of the E-field strength in V/m vs frequency is generated and the max value in dBm from each file is displayed in the appropriate Edit Box. Pressing the "Calculate" button the results of the post processing of the measurement data are calculated and compared with the respective limits of exposure, and the corresponding graph is created.

All variables that can affect the measurements, such as the change of characteristics of the SA, the antenna factor data, the cable attenuation data etc., after newer calibration of the used instrumentation, have been registered in respective databases, in order to change the corresponding values easily. Finally, the "Report" button automatically creates the report of the Radar measurements in a Microsoft Word file for appropriate use. The Report was written according to ELOT 1422-3. From this GUI we can also view the Occupied Bandwidth of the Radar which was calculated during the process of this work, the documentation, the master thesis document for this work and the theoretical calculations for Radar transmission. In the menu of the post processing GUI, the choice of Channel Power can be selected. This function opens a new GUI, which concerns the Channel Power method for measuring Radar. This method is described in chapter 8 in this document. Also, if the exposure ratio λ is greater or equal to 1 then the Radar emission is an emission above the exposure limits. In this case, the corresponding values of λ and E_{peak}, E_{av}, S_{peak}, S_{av} in the GUI figure are displayed in red color. In Fig. 7.4 an example with λ=1 is shown (this is only an example of the operation of the post processing program and not a calculation from real measurements). In Fig. 7.5 the flow chart of the post processing GUI is presented.

Figure 7.3 The post processing GUI

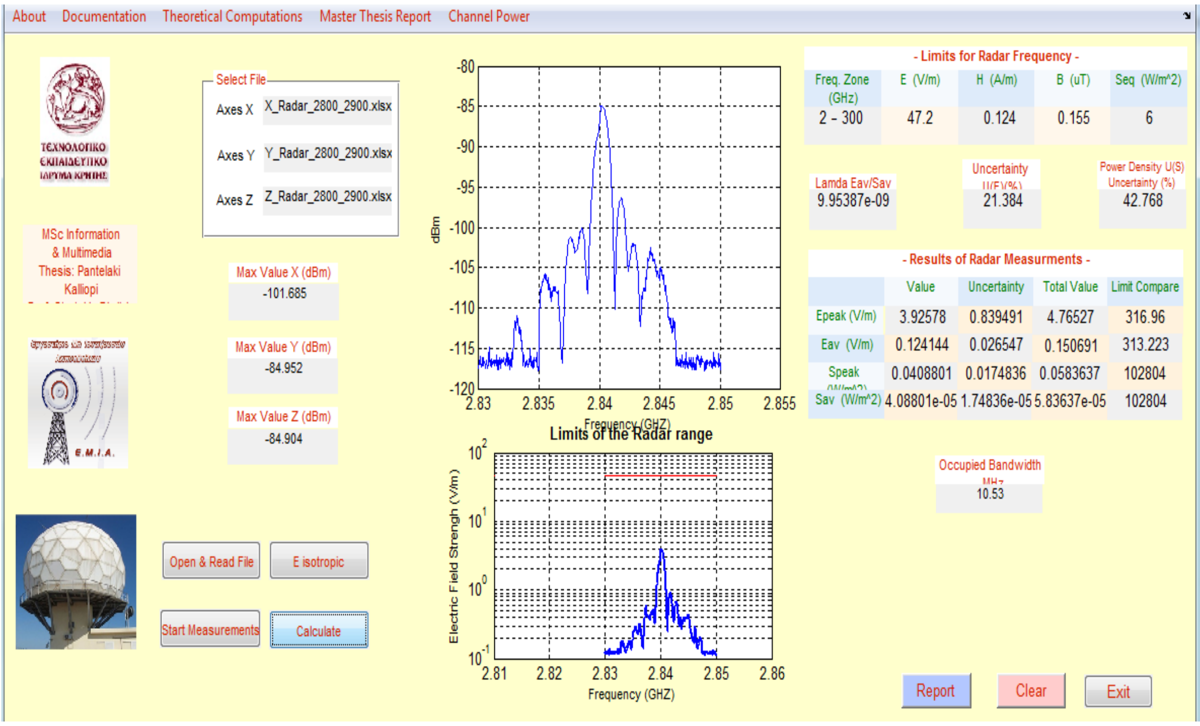

Figure 7.4 Example with λ >=1

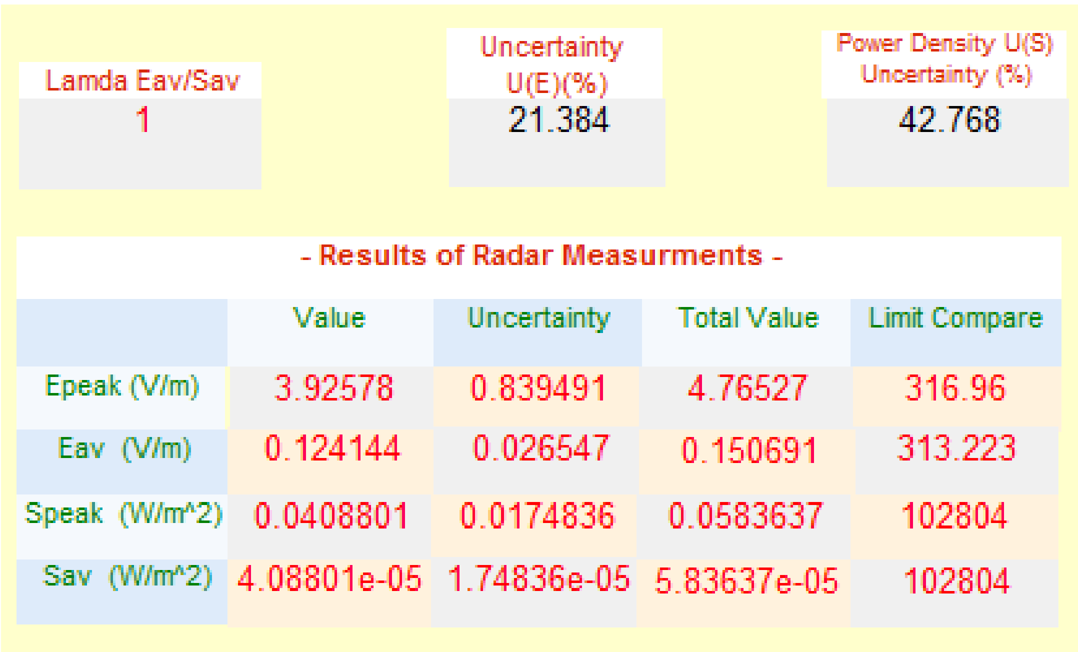

Lamda Eav/Sav	Uncertainty U(E)(%)	Power Density U(S) Uncertainty (%)
1	21.384	42.768

- Results of Radar Measurments -

	Value	Uncertainty	Total Value	Limit Compare
Epeak (V/m)	3.92578	0.839491	4.76527	316.96
Eav (V/m)	0.124144	0.026547	0.150691	313.223
Speak (W/m^2)	0.0408801	0.0174836	0.0583637	102804
Sav (W/m^2)	4.08801e-05	1.74836e-05	5.83637e-05	102804

Figure 7.5 Flow chart of the processing GUI

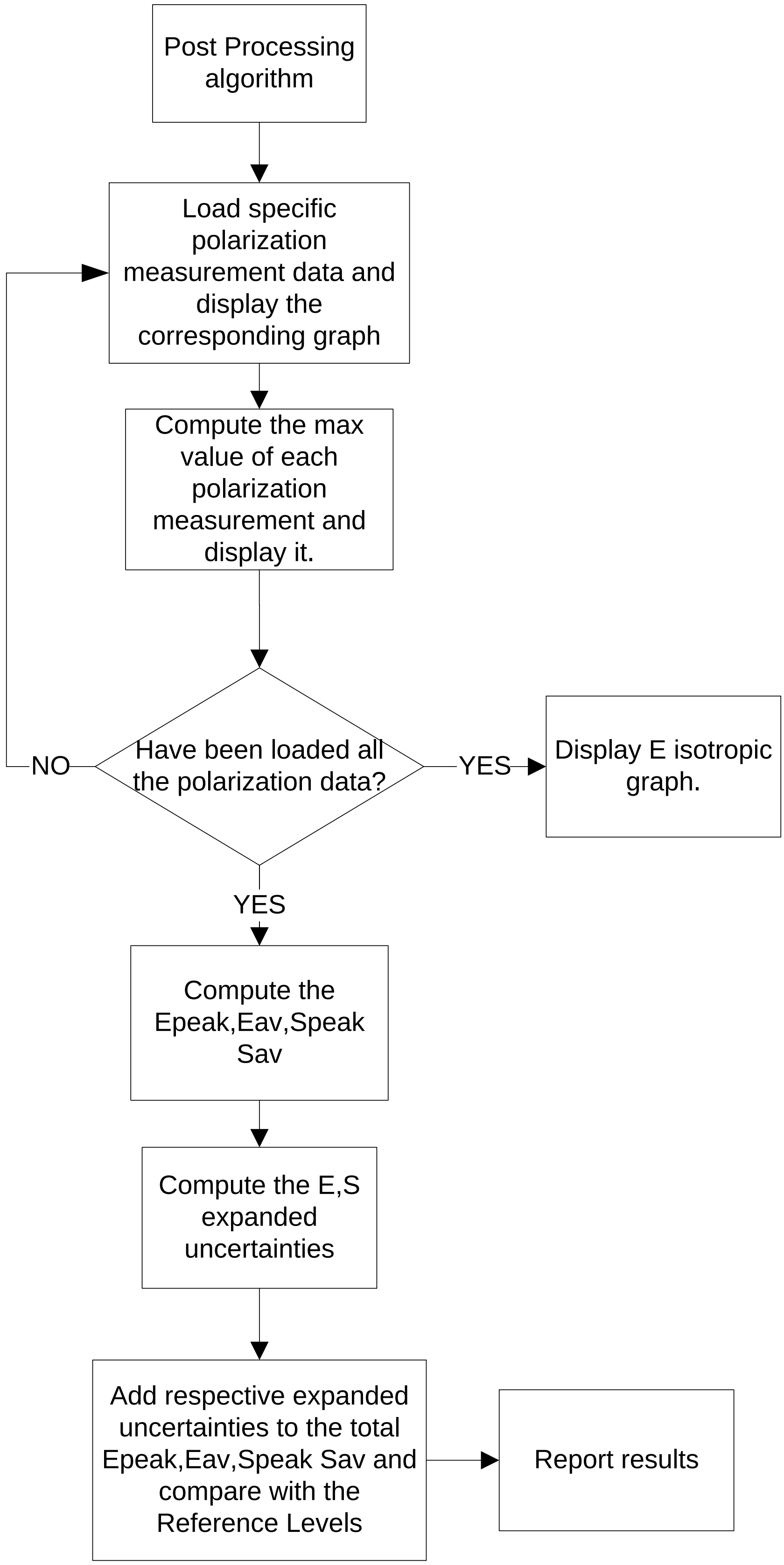

Chapter 8 -Radar measurements with Channel Power method

In this work, Radar measurements were made with a different manner than that of the spectrum mode of SA. These measurements were carried out with a non automatic method. The place which was chosen for these measurements is at the TEI of Heraklion, near the NIR laboratory. This point is not in line of sight with the Radar but we choose this point only for testing purposes. In this study, the Occupied Bandwidth (OBW) of the Radar signal is measured fist of all and after that Radar measurements were made with the Channel Power function of SA. In order to compare the two methods of measuring the Radar, the spectrum mode of SA and the Channel power function of SA, spectrum mode measurements were also carried out in this place.

8.1 Occupied Bandwidth

Occupied bandwidth of the signal is the bandwidth containing 99.0% of the signal's total power. To make the measurement of OBW we make the following settings in the spectrum analyzer [32]:

Span: 40 MHZ
Resolution bandwidth (RBW): 1 MHz
Video bandwidth (VBW): 3 MHz
Detector: Max Peak
Trace: MaxHold
Channel Bandwidth: 5 MHZ

Measurements Result: OBW = 10.53 MHz

Figure 8.1 Occupied bandwidth measurement

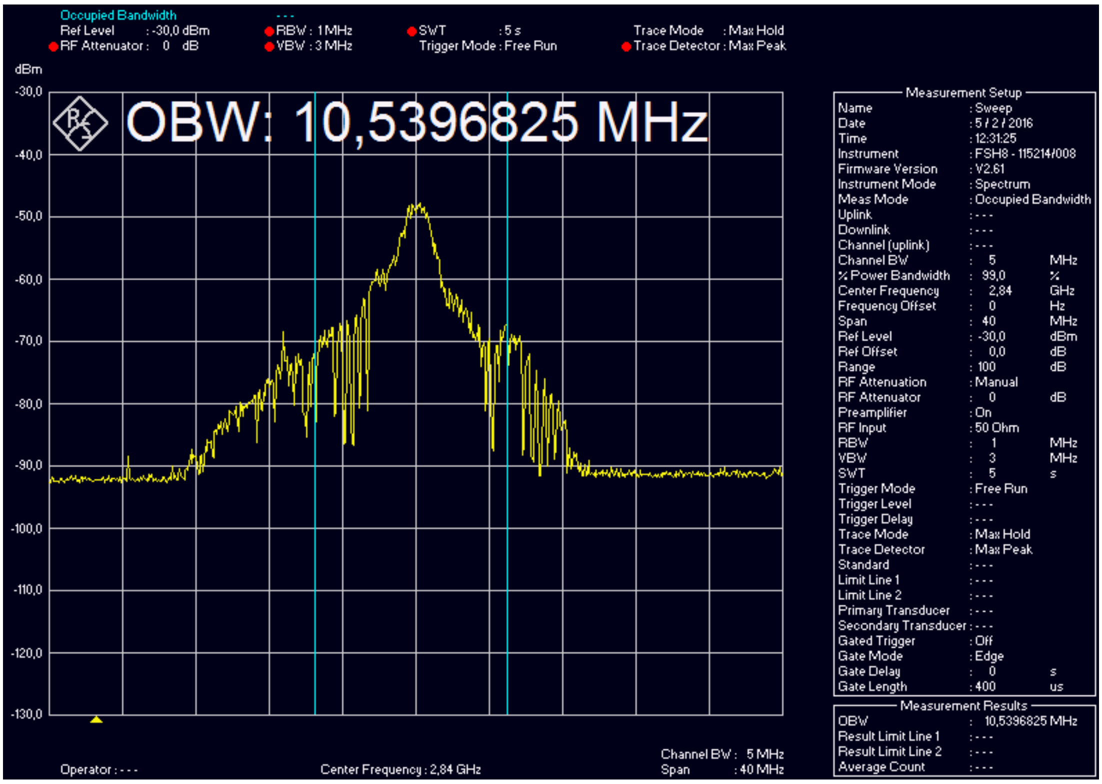

8.2 Spectrum mode measurements

The measurements and the evaluation of the Spectrum mode measurements carried out in the manner described in chapter 6. The collection of measurements and the processing software were used. So, the results are:

Xmax = -103.94 dBm

Ymax = -94.73 dBm

Zmax = -95.33 dBm

The calculations of E_{peak} , E_{av}, S_{peak}, S_{av} and the results of the comparison with the limits are shown in figure 8.2, as the post processing software is given. Figure 8.3 illustrates the E field strength isotropic graph.

Figure 8.2 The results of the comparison with the limits

Lamda Eav/Sav	Uncertainty U(E)(%)	Power Density U(S) Uncertainty (%)
1.02525e-09	21.384	42.768

- Results of Radar Measurments -

	Value	Uncertainty	Total Value	Limit Compare
Epeak (V/m)	1.25993	0.269423	1.52935	987.608
Eav (V/m)	0.0398424	0.00851992	0.0483624	975.966
Speak (W/m^2)	0.00421066	0.00180082	0.00601148	998090
Sav (W/m^2)	4.21066e-06	1.80082e-06	6.01148e-06	998090

Figure 8.3 E field strength isotropic graph

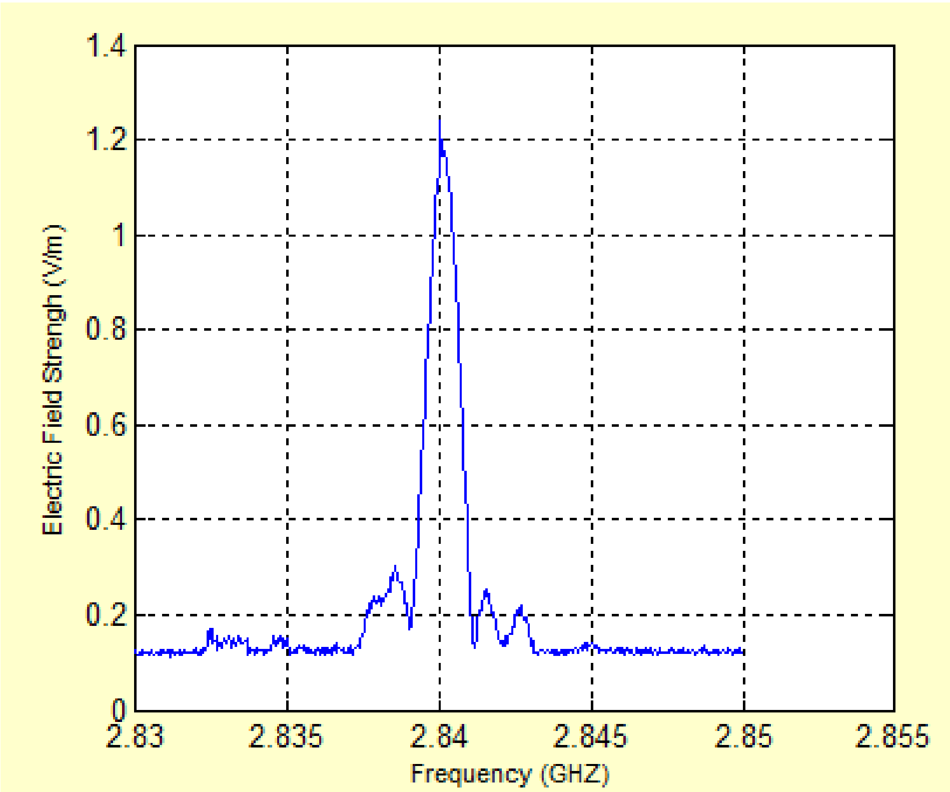

So, $E_{peak} = 1.53$ V/m $\quad S_{peak} = 0.006$ W/m^2

$E_{av} = 0.048$ V/m $\quad S_{av} = 6.067 \times 10^{-6}$

8.3 Channel Power

With Channel Power function we can measure the average power across the frequency band of interest [29]. The Channel Power function is very useful when we measure pulsed radar because it has complex signals and often the PRF and the pulse width are changed. Thus, the spectrum of these signals is also complex and the power cannot be easily calculated from the spectrum [31] [47].

Radar measurements with the channel power method were carried out with the same measurement system as the spectrum mode. So, in order to simulate an isotropic reception of the fields, measurements were made in three mutually perpendicular polarizations (X, Y and Z). We make the following settings in the spectrum analyzer for these measurements [30] :

Span: 20 MHZ
Resolution bandwidth (RBW): 30 KHz
Video bandwidth (VBW): 300 KHz
Sweep Time: 5 sec
Detector: RMS
Trace: MaxHold
Channel Bandwidth: 10 MHZ

Measurement Results: XPower = -83.4 dBm
YPower = -84.9 dBm
ZPower = -88.3 dBm

The figure 8.4 illustrates the channel power measurements.

Figure 8.4 Channel Power measurements

X Polarization Xpower = -83.4 dBm

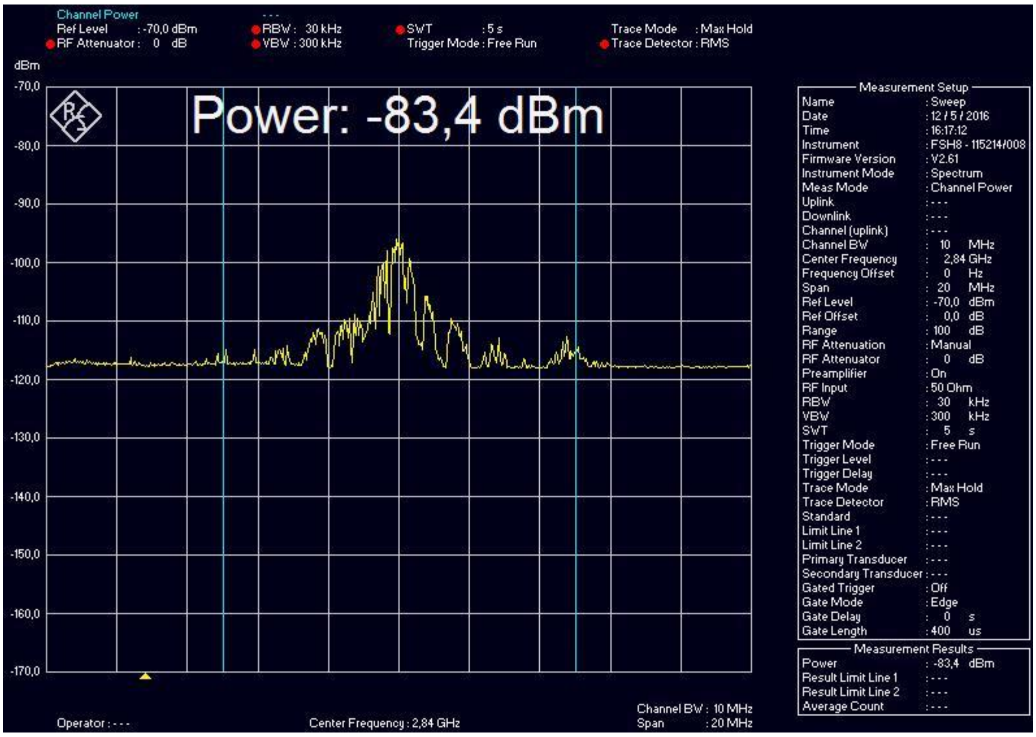

Y Polarization Ypower = -84.9 dBm

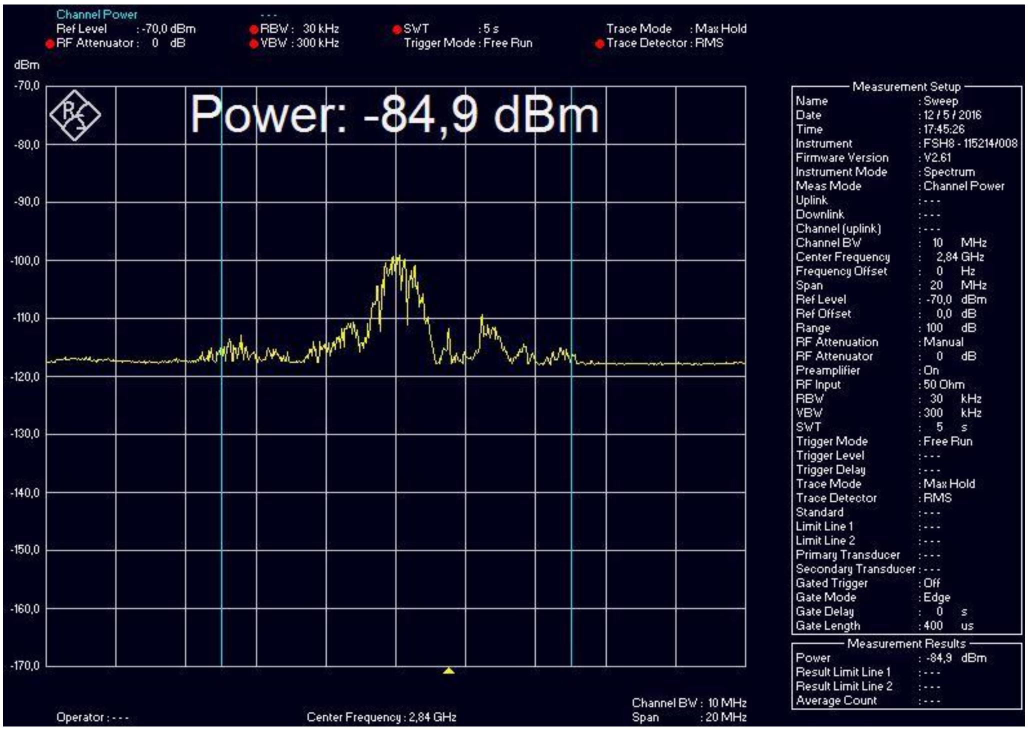

Z Polarization Zpower = -88.3 dBm

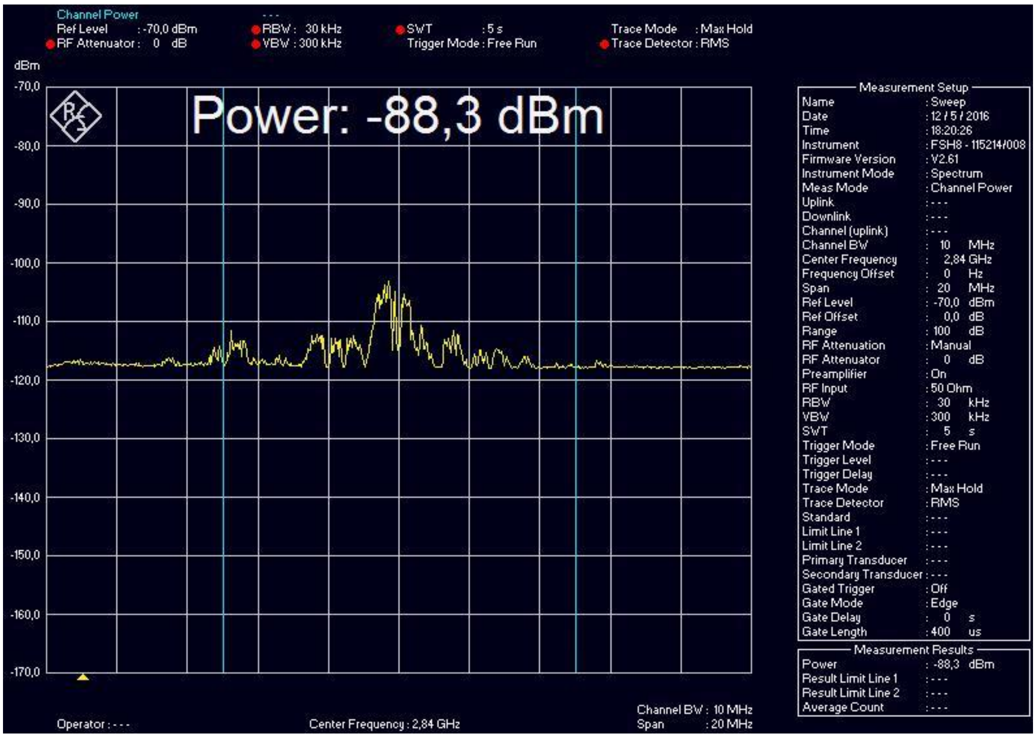

Peak pulse power was traditionally determined by measuring the average power of the pulse and then dividing the measurement result by the pulse duty cycle value (figure 8.5), as shown [48] [49]:

$$P_{peak} = \frac{P_{av}}{duty\ cycle}$$

Figure 8.5 Peak and average power measurement

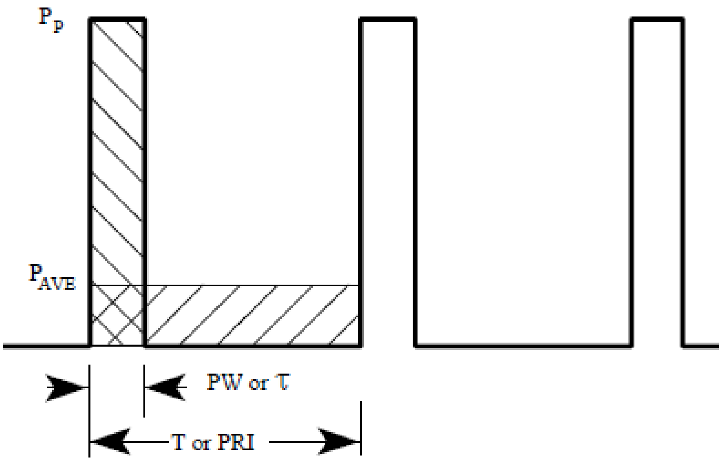

According to [50] we have:

$$P_{in}(f_i) = P_i + P_c + \sum_{j=1}^{m} L_{ji} - G_{dB}(f_i)$$

<u>Measurement System (MS) Losses:</u>

Connectors = 0.3 db

Both PCD Cables Attenuation (third order splines algorithms were used) = 11.71 dB

Total loss = 12,01 db.

<u>G, antenna gain:</u>

AF = 20logf – G – 29.8 dB/m, f in MHz, AF = 44.83 dB/m (third order splines algorithms were used)

G db = - AF + 20log2840 – 29,79 = - 44,83+69,06 – 29,79= - 5.56 db.

$\sum_{j=1}^{m} L_{ji} - G_{dB}(f_i)$ = 12.01- (-5.56) = 17.57 dB

The power density at the input of MS at the X polarization is:

$S_{in,x,dB}$ = -83,42+17,57 = -65.85dBm

The power density at the input of MS at the Y polarization is:

$S_{in,y,dB}$ =-84,9+17,57= -67.33dBm

The power density at the input of MS at the Z polarization is:

$S_{in,z,dB}$ =-88,3+17,58= -70.73 dBm

The table 8.1 shows the calculations of S, E for each polarization.

Table 8.1 Channel Power calculations for each polarization

	$S_{in,x,dB}$	$S_{in,y,dB}$	$S_{in,z,dB}$
	-65.85	-67.33	-70.73
S (W/m²)	2,60E-06	1,85E-06	8,47E-07
E (V/m)	0,031	0,026	0,017

We know:

$S_{in}(f_i) = 10 * 10^{\frac{SindBm(fi)}{10}}$ W/m²

So, we have:

E_{av} V/m = $\sqrt{Ex^2 + Ey^2 + Ez^2} = 0.044$ V/m

$S_{av} = \frac{Eav^2}{377} = 5.3 * 10^{-6}$

The uncertainty of the measurement system.

The measurement system in this method of measurement remain the same as the spectrum mode method but we have to add the factor u($_{cfB}$) to the combined standard uncertainty u_c in each polarization due to the channel method [42]. We have:

$$u(_{cfB}) = \sqrt{(\frac{1}{2}\frac{u(span)}{Span})^2 + (\frac{1}{2}\frac{u(RWB)}{RWB})^2}\ 100\% = 0.025100\%$$

So, the combined standard uncertainty u_c in each polarization is:

$$u(E_{pi}) = \sqrt{\sum_{i=1}^{N} u^2{}_{(xi)+u(cfB)^2}} = 10.9\ \%\,.$$

the same value with the spectrum mode method.

So, we have:

Expanded uncertainty U($_E$) = **21.38%**

The Expanded uncertainty U(S) is: U(S) = **42.76%**

E_{av} = 0,044 V/m with the uncertainty U($_E$) = **21.38%** :

0.044*21.38/100=0,009 V/m.

E_{av} = 0,044+0,009 = 0,053 V/m

E_{av}: 47,2/0,053= 890.56 times below the corresponding limit.

S_{av} = $5.3 * 10^{-6}$ W/m^2 average with the uncertainty U($_S$) = **42.76%** :

S_{av} = $5.3*10^{-6}*42.76/100 = 2.26*10^{-6}$ W/m^2

S_{av} = $5.3*10^{-6} + 2.26*10^{-6} = 7.56*10^{-6}$ W/m^2

S_{av} : $6 / 7.56*10^{-6}$ = 792992.06 times below the corresponding limit.

So, if we compare both methods of measurements of Radar, we can see that the results are almost the same.

In this work, we can also calculate the E_{peak}, S_{peak} for the PSR Radar using the formula: $E_{Peak} = \frac{Eav}{\sqrt{Duty\ Cycle}}$, with Duty cycle = 0.001.

So, E_{Peak} = 0.044/0.001 = 1.39 V/m,

Expanded uncertainty $U(_E)$ = **21.38%**

E_{peak} = 1.39 V/m with the uncertainty $U(_E)$ = **21.38%** :

1.39*21.38/100=0,29 V/m.

E_{peak} = 1.39+0,29 = 1.68 V/m

E_{peak}: 32*47,2/1.68= 899.04 times below the corresponding limit.

$S_{peak} = E_{peak}^2 / 377 = 1.39^2 /377 = 0.0051$ W/m^2

The Expanded uncertainty U(S) is: U(S) = **42.76%**

0.0051*42.76/100 = 0.002 W/m^2

S_{peak} = 0.005+0.002 = 0.007 W/m^2

S_{peak} : 6000/0,007 = 843327.38 times below the corresponding limit

Figure 8.6 shows the channel power GUI from the post processing program, as the two methods of measuring Radar can easily be compared.

Figure 8.6 The post processing Channel Power GUI

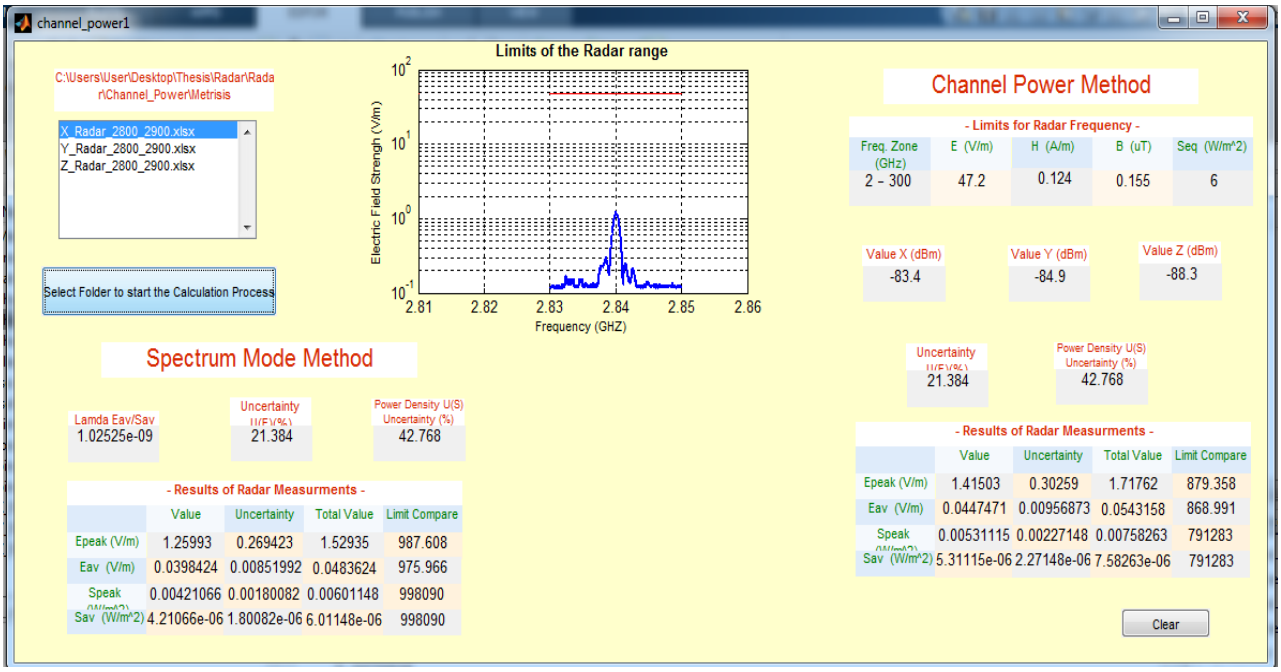

Figure 8.7 Photos during measurement process

Chapter 9 - Conclusions & Future Work

In this work measurements for the estimation of the electromagnetic burden of the Surveillance Radar (PSR) of Nikos Kazantzakis airport of Heraklion, Crete were made for testing purposes. Since Radar is a special electromagnetic emission source due to the pulse transmitted signals and their rotations, the measurements of the electromagnetic fields produced must be made with the appropriate settings of narrowband receivers like Spectrum Analyzers (Narrow-band measurements). The appropriate equipment of the Non Ionizing Radiation Laboratory (NIRL) of Technological Educational Institute of Crete was used. The place which was chosen for the measurements is close to TEI at Heraklion and it is in line of sight with the Radar. For this purpose, two dedicated software programs were developed in the MATLAB environment, one for the remote control of the used instrumentation and the collection of the measurement data and the other for the processing of them. The great benefit is that all the appropriate instrumentation settings can be incorporated in the software, resulting in less risk of mishandling. Moreover, the analysis of the measurement data requires the proper corrections to be taken into account so that the evaluated exposure values can be compared with the respective exposure limits. The two dedicated software programs include Graphical User Interfaces (GUI) for easier handling of the appropriate settings and calculations.

The measurement manner, the instrument settings and the processing of the measurements were made after a detailed study and literature review of a lot of relative works and applications in this domain. The measurements were made with the Spectrum mode of the SA.

The results from post processing the measurement data showed that Heraklion PSR Radar radiation is within the safety limits at the measurement point.

Except the automatic manner for collection and processing the PSR measurements, other non automatic manner measurements for the PSR Radar were carried out with the Channel Power function of SA. For this purpose, new measurements with the automatic manner were made inside the place of TEI of Crete at Heraklion and near the Non Ionizing Radiation Laboratory. After that, channel power measurements were collected. The evaluation of the two measurement manners showed that the results were comparable. Also, the Occupied Bandwidth of Heraklion PSR Radar was measured in a non automatic manner.

Future work may introduce more automation options to the presented software in order to avoid operator mistakes and make the Radar evaluation of exposure easier. The Occupied Bandwidth measurements, the channel power measurements or other methods for dedicated Radar measurements can be added to this software. This is very important because the new PSR Radars will be more complex and vary their PRF or pulse width. So, the measurement power cannot be so easily derived from the spectrum.

Furthermore, Radar signal analysis, processing, and Radar system design can be achieved by using the Matlab program [51] [52] [53]. In this manner, a Radar simulation program can be created and after that the methods of measuring Radar and the characteristics of Radar pulse signal can be verified.

References

[1] (2015, December) NASA. [Online]. http://imagine.gsfc.nasa.gov/science/toolbox/emspectrum1.html

[2] (2015, December) World Health Organization. [Online]. http://www.who.int/ionizing_radiation/about/what_is_ir/en/

[3] narda Safety Test Solutions, "NON-IONIZING RADIATION GENERAL INFORMATION," *Application Note*, pp. 100-107.

[4] S. Bandyopadhyay and S. Ganguly S. Banik, "Review paper Bioeffects of microwave––a brief review," *Bioresource Technology- Elsevier Science Ltd*, pp. 155-159, 2003.

[5] et al P. Vecchia, "Exposure to high frequency electromagnetic fields, biological effects and health consequences (100 kHz-300 GHz)," *ICNIRP*, 2009.

[6] L.J. Challis, "Review: Mechanisms for Interaction Between RF Fields," *Bioelectromagnetics Supplement- Wiley InterScience*, pp. 98-106, 2005.

[7] I. Belyaev, "Non-thermal Biological Effects of Microwaves," pp. 13-29, November 2005.

[8] J. M. Williams, "Biological Effects of Microwaves:Thermal and Nonthermal Mechanisms," *Biological Thermal and Nonthermal Mechanisms*, vol. V.44, pp. 1-48, August 2013.

[9] (2015, December) Home page eett. [Online]. http://www.eett.gr

[10] World Health Organization, "IARC CLASSIFIES RADIOFREQUENCY ELECTROMAGNETIC FIELDS AS," WHO, Lyon, France, No 208, 2011.

[11] C. Sage L. Hardell. (2007, December) sciencedirect. [Online]. www.sciencedirect.com

[12] Barbora V. and J. Vrba J. Vorlíček. (2011, November) Home page Intechopen. [Online]. www.intechopen.com

[13] WHO. (2016, January) Home page WHO. [Online]. http://www.who.int/peh-emf/publications/facts/fs226/en/

[14] K. R. Foster, "Thermal and Nonthermal Mechanisms of Interaction of Radio-Frequency Energy with Biological Systems," *IEEE TRANSACTIONS ON PLASMA SCIENCE*, vol. VOL. 28, no. NO. 1, pp. 15-23, FEBRUARY 2000.

[15] INTERNATIONAL COMMISSION ON NON-IONIZING RADIATION PROTECTION (ICNIRP), "ICNIRP GUIDELINES FOR LIMITING EXPOSURE TO TIME-VARYING ELECTRIC, MAGNETIC AND ELECTROMAGNETIC FIELDS (UP TO 300 GHZ)," ICNIRP, HEALTH PHYSICS 74 (4):494-522; 1998, 1998.

[16] Sage rerort. (2016, January) Homepage Sage rerort. [Online]. http://sagereports.com/smart-meter-rf/?page_id=216

[17] Merill Skolnik, *Radar Handbook*, Third Edition ed.: McGraw-Hill Companies, 2008.

[18] Agilent, "Radar Measurements," Agilent Technologies, USA 5991-7575EN, 2014.

[19] D. Stratakis1, T. Xenos2, V. Zacharopoulos1 A. Miaoudakis1, "Human Electromagnetic Exposure Compliance to Radar Systems," in *TEMU*, 2010, p. 7.

[20] British Ministry of Defence, "GUIDE TO THE PRACTICAL SAFETY ASPECTS OF THE USE OF RADIO FREQUENCY ENERGY," Ministry of Defence, O5 - 74/Issue 1, 1989.

[21] Dr. Rainer Bitzer, "BROADBAND FIELD STRENGTH MEASURING SYSTEM UP TO 18GHZ," *Compliance Engineering*, p. 7, 1997.

[22] J. Barfuss, "Perfecting Pulsed RF Radar Measurements," *Applications Engineer,Agilent Technologies*, p. 4, August 2007.

[23] Werner Schaefer, "NARROWBAND AND BROADBAND DISCRIMINATION with spectrum analyzer and EMI receiver," *IN Compliance*, pp. 1-21, December 2010.

[24] Blake Peterson, "Spectrum Analysis Basics. Applicat ion Note 150," *Agilent Technologies*, 2013.

[25] Agilent Technologies, "Spectrum and Signal Analysis…Pulsed RF. Application Note 150-2," *Agilent Technologies*, 2012.

[26] G. Miaris et al, "Design of Radiation-Emission Measurements of an Ai r-Traff ic S u rvei I lance Radar," *IEEEAnfennas and Propagation Magazine*, vol. Vol. 45, no. No. 4, pp. 35-46, August 2003.

[27] C. J. Veranopoulos, Prof. Ph. Constantinou A.D. Marousis, "Radiation Intensity for the Approach RADAR at 'N. Kazantzakis' Airport, Heraklion, Crete," in *Applied Electromagnetism, 2000. Proceedings of the Second International Symposium of Trans Black Sea Region on* , Xanthi, 2000.

[28] David A. Hall. (2016, February) electronic design. [Online]. http://electronicdesign.com/test-measurement/zero-span-made-simple

[29] Agilent Technologies, "Agilent Spectrum and Signal Analyzer Measurements and Noise 5966 4008," Agilent Technologies, USA 5966 4008, 2012.

[30] Christoph Rauscher et al, "Fundamentals of Spectrum Analysis," Rohde & Schwarz GmbH & Co. KG, Germany, 2001.

[31] Rohde&Schwarz FSP, "Power Measurement on Pulsed Signals with Spectrum Analyzers," Rohde&Schwarz FSP, Germany, 1EF48_2E, 2003.

[32] ITU-R, "Bandwidth measurement at monitoring station.," ITU, Recommendation SM.443-3, 2005.

[33] Narda Safety Test Solutions GmbH, "Radar measurements with the Selective Radiation Meter SRM-3000," Meter SRM-3000, Application Note AN_HF_1003_Radar_Measurements, 2007.

[34] Greek legislation, "How to perform measurements for compliance with the safety exposure limits public to electromagnetic radiation from each antenna.," 346/2008, 2008.

[35] UKAS, "The Expression of Uncertainty in EMC Testing," UKAS, LAB34, 2002.

[36] BIPM, "Evaluation of measurement data — Guide to the expression of uncertainty in measurement," JCGM 100:2008, 1995.

[37] GREEK ORGANISATION STANDARDS, "HELLENIC STANDARD ," Athens, ICS: 33.020 / ΕΛΟΤ 1422-3, 2006.

[38] Agilent Technologies, "Power Measurement Basics,".

[39] Electronic Communications Committee (ECC), "ECC RECOMMENDATION (02)04 MEASURING NON-IONISING ELECTROMAGNETIC RADIATION (9 kHz – 300 GHz)," ECC/REC/(02)04, 2003.

[40] UKAS, "The Expression of Uncertainty and Confidence in Measurement ," United Kingdom Accreditation Service, M3003/ Edition 2, 2007.

[41] A. Miaoudakis, V. Zacharopoulos and T. Xenos D. Stratakis, "On the Spatial Averaging of Multiple Narrowband Electromagnetic Field Measurements. Methods and Uncertainty Estimation," *IEEE Trans. Instrum. Meas.*, vol. 59, no. 6, pp. 1520-1536, June 2010.

[42] A. Miaoudakis, T. Xenos and V. Zacharopoulos D. Stratakis, "Overall Uncertainty Estimation in Multiple Narrowband in Situ Electromagnetic Field Measurements ," *IEEE Trans. Instrum. Meas.*, vol. 58, no. 8, pp. 2767-2779, Aug 2009.

[43] Greek legislation, "Common Ministerial Decision-Protection measures for the exposure of the general public to all land based antenna stations," Act No.1105/Vol. B, 6-9-2000.

[44] Greek legislation, "Law 3431, About Electronic Communications and other orders," Act No.13/Vol. A, 3-2-2006.

[45] K.G. Pantelaki et al, "Radar Measurements with Remote Control Software," in *TEMU*, Heraklion, 2016, pp. 1-6.

[46] SCPI Consortium, "Standard Commands for Programmable Instruments (SCPI)," USA, Volume 1: Syntax and Style, May 1999.

[47] Rohde & Schwarz, "Tackling the Challenges of Pulsed Signal Measurements," Rohde & Schwarz, Application Notes 1MA124_0E, 2008.

[48] Agilent Technologies, "Making Accurate Radar Pulse Power Measurements," USA, Application Notes 5991-2643EN, 2013.

[49] Mastering Electronics Design. (2016, June) Mastering Electronics Design. [Online]. http://masteringelectronicsdesign.com/how-to-derive-the-rms-value-of-pulse-and-square-waveforms/

[50] et al D. Stratakis, "Automation in Electromagnetic Field Measurements," in *Proceedings of the International Conference on Telecommunications & Multimedia, ISBN: 960-88785-2-7*, Heraklion, Crete, Greece, TEMU 5-7 July 2006 , pp. 1-6.

[51] Bassem R. Mahafza, *RADAR SIGNAL ANALYSIS AND PROCESSING USING MATLAB*. Alabama, U.S.A.: CRC Press, Taylor & Francis Group, 2009.

[52] CANER ÖZDEMI˙R, *Inverse Synthetic Aperture Radar Imaging with MATLAB Algorithms*. Canada: Wiley, 2012.

[53] Bassem R. Mahafza, *Radar Systems Analysis and Design Using MATLAB*. USA: CHAPMAN & HALL/CRC, 2000.

Appendix A - Spectrum Analyzer figures of display at the end of measurements.

The figures of SA display at the end of measurements.

Figure A.1 The figures of SA display

X polarization

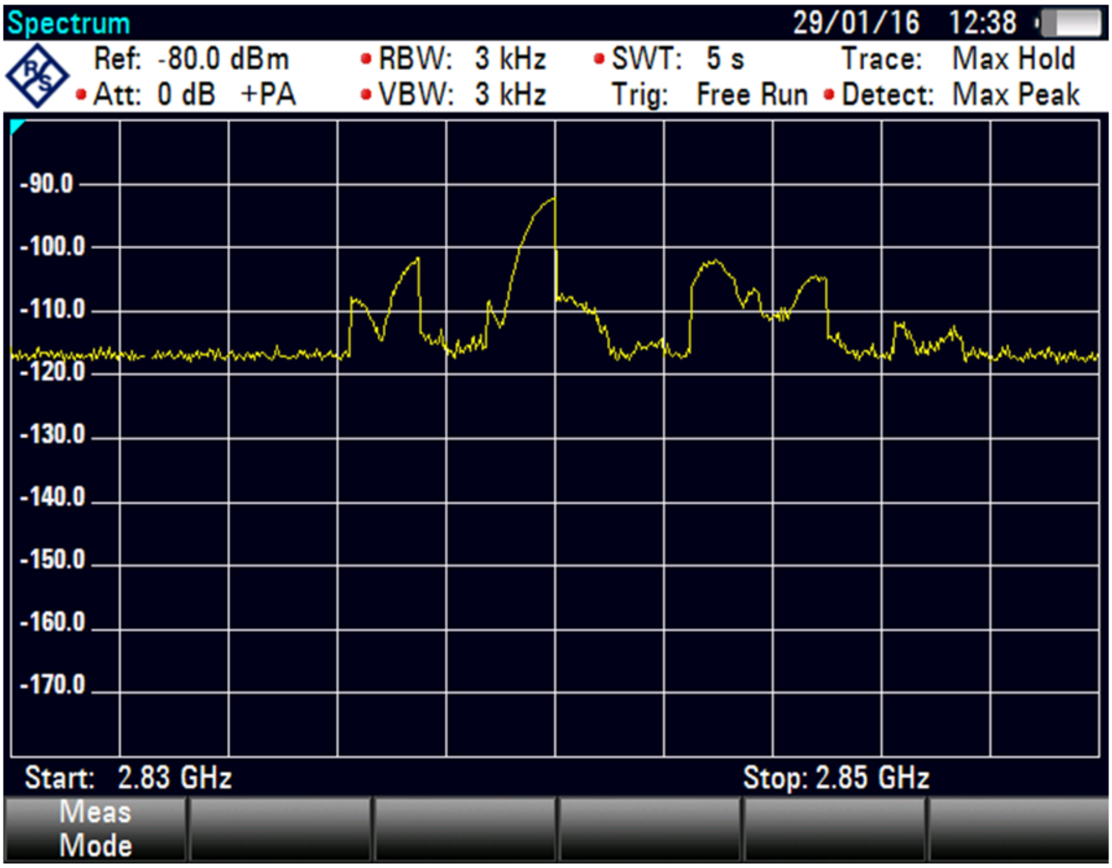

Y polarization

Z polarization

The Radar Pulse in time domain. The Zero span mode of SA was used.

Figure A.2 The Radar Pulse in time domain

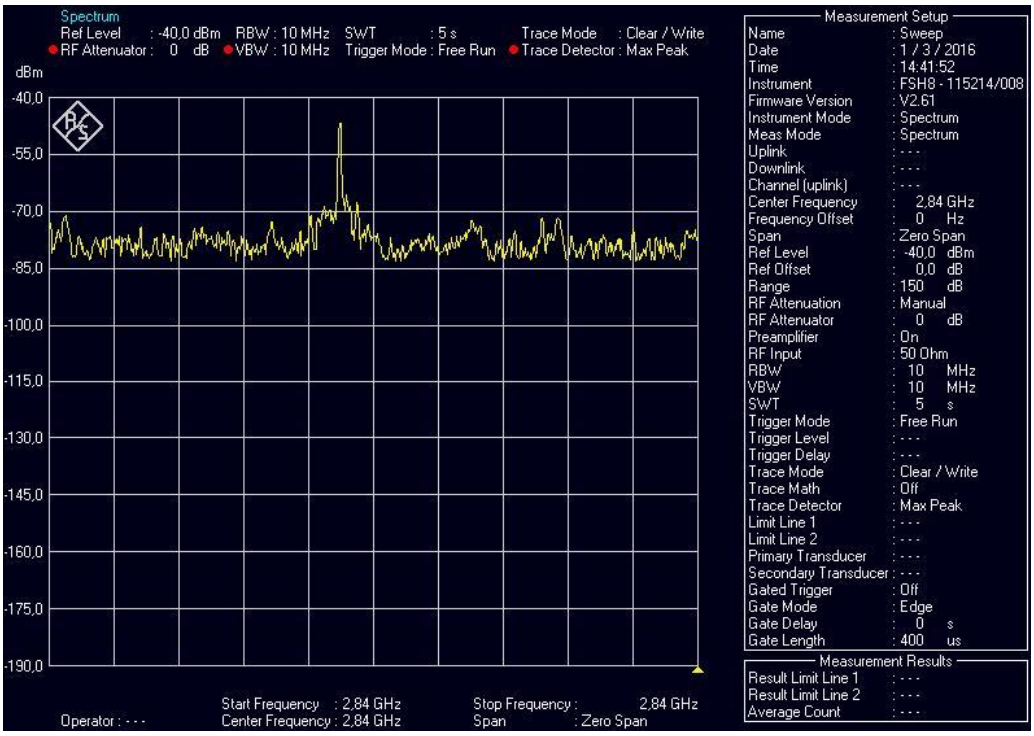

Appendix B - The Report from the processing GUI

Date of report creation: 07-Jun-2016_ 20:38

Postgraduate program

“Informatics and multimedia”

Technological Educational Institution (TEI) of Crete

Report

Measurements of the electromagnetic radiation emitted by the civil aviation Primary Surveillance Radar (PSR) of Nikos Kazantzakis airport of Heraklion, Crete.

Author: Pantelaki Kalliopi

1. History

Within the framework of the thesis of Kalliopi Pantelaki for the postgraduate program "Informatics and multimedia" of the Technological Educational Institution (TEI) of Crete, measurements of electromagnetic radiation emitted by the civil aviation PSR of the Nikos Kazantzakis airport, were made for experimental purposes.

The measurements were performed using the equipment of the Non Ionizing Radiation Laboratory (NIRL) of the Technological Educational Institute of Crete. All devices are accompanied by certificates of quality, calibration and excellent operation. For the collection and processing of these measurements the appropriate software was developed. All measurement results are saved on a laptop PC.

2. Characteristics of the emitter

The Primary Surveillance Radar of the Nikos Kazantzakis airport is located in Dyo Aorakia area of the Municipality of Heraklion. Geographical position: 35 19'39.50'' N 25 10' 21.36''E. It belongs to the Hellenic Civil Aviation Authority. This radar includes two transmit channels operating at the frequency 2840 MHz and 2760 MHz. During measurements, the transmit channel was set to 2840 MHz. Hellenic statutory transmit emission standards in the frequency band of the radar (KYA 53571/3839/2000, Law: 3431/2006) are: For frequencies 2 – 300 GHz we have Electric Field Intensity E = 47,2 V/m and Equivalent Density Sequence Seq = 6 W/m^2.

People responsible for the Measurements:

Dr. Dimitrios Stratakis: Assistant Professor, Department of Informatics Engineering, TEI of Crete

Kalliopi Pantelaki, Postgraduate student

Date of measurements: 29/1/2016

3. Measurement equipment

Measurement System

All measurements of electromagnetic quantities mentioned in this report were made using the necessary equipment from the Non Ionizing Radiation Laboratory (NIRL) of the Technological Educational Institute of Crete, Department of Informatics Engineering.

The equipment used is:

- Spectrum analyzer (SA): ROHDE & SCHWARZ FSH8 – Spectrum analyzer 9 KHz to 8 GHz.
- Antenna Rotator
- Two RF cables
- One Laptop
- Antenna tripod
- Special designed software in Matlab platform to serve this research. This software has two parts. One is used for the collection of measurement data and the other for the processing of these data.

All devices used in this laboratory are accompanied by certificates of quality, calibration and excellent operation.

4. Procedure of measurements and evaluation of exposure to electromagnetic fields.

All measurements were made according to the report and the directions from Narda application node “Radar measurements with the Selective Radiation Meter SRM-3000”.

The measurement settings for spectrum analyzer are the following:

- Center frequency: 2840MHz (or 2760MHz)
- SPAN: 20MHz
- Operational Mode of SA: Spectrum Mode
- Trace Mode: MAX HOLD
- Detection Mode: Positive peak
- RBW >PRF: 3 KHz
- VBW >=RBW: 3KHz
- Sweep time > Trot: 5 sec (Trot Radar=4 sec)

The measurement duration was 30 minutes.

Using the measurement software we made measurements in the three antenna polarization axis X, Y, Z, since an omnidirectional antenna is not available. All these measurements were saved in three MS Excel files.

In order to calculate the uncertainty of the measurements, we used the methods proposed in [1], [2], [3]. For the used antenna and cables, the antenna factor and the calibration certificates of cable attenuation are taken into account. The expanded measurement uncertainty is calculated with a 95% coverage probability and coverage factor k = 1.96 (normal distribution).

Furthermore, with the help of the developed software we are processing all measurement results and compare them with the corresponding limits of exposure. From each of the three measurement files the maximum value was selected. Each max value was corrected with the total instrumentation losses (cable and connector losses) and the antenna gain value in order to calculate the maximum received power at the place of the receiving antenna. Then, the received power was converted to electric field strength, and the value of the electric field strength was corrected according to equation ap = 20*Log(teff *k*RBW) (where αp is the desensitization factor, teff is the pulse width in seconds, RBW is the resolution bandwidth in Hz and the value of k is given by the manufacturing company of the used SA) in order to evaluate the maximum received electric field for each polarization (X, Y and Z). The maximum total field strength is calculated by the root sum of the squares (RSS) of the three calculated E - field components according to the following equation:

$$|E_{total}| = \sqrt{E_x^2+E_y^2+E_z^2}$$

where: Ex, Ey and Ez are the three calculated components of the electric field strength at the three antenna polarizations. For human exposure from pulsed emissions, the average of Seq (W/m^2) throughout the pulse width should not exceed 1000 times the respective RLs. Also, the field strength values must not exceed 32 times the RLs for the respective field strength. We take further into consideration the measurement uncertainty and we compare the total maximum received electric field strength with the Hellenic statutory transmit emission standards in the frequency band of the radar.

The relation between power density, electric field strength in the far field region of an antenna is given by: S = E^2/n, where: n = 120*π = 377Ohms is the characteristic resistance of free space.

Power spectrum of Nikos Kazantzakis PSR

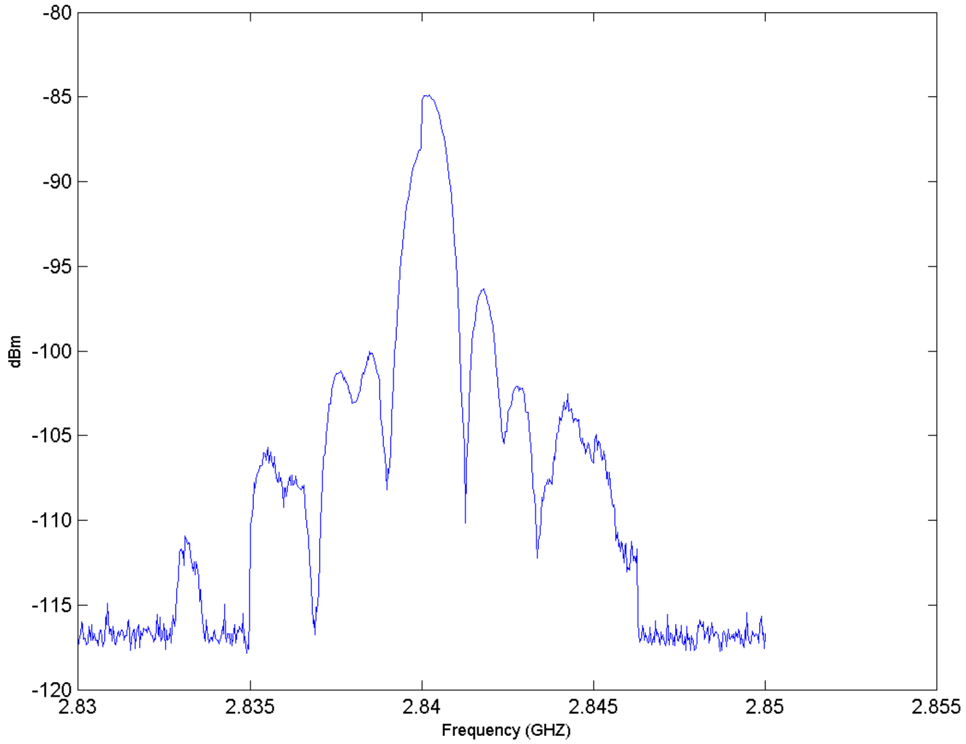

5. Measurement station

The place which was chosen for the measurements is close to TEI of Heraklion and it is in line of sight with the Radar. Geographical position: 35 19’41.80’’ N 25 09’ 51.98’’E.

Measurement point

6. Conclusion

The post processing GUI

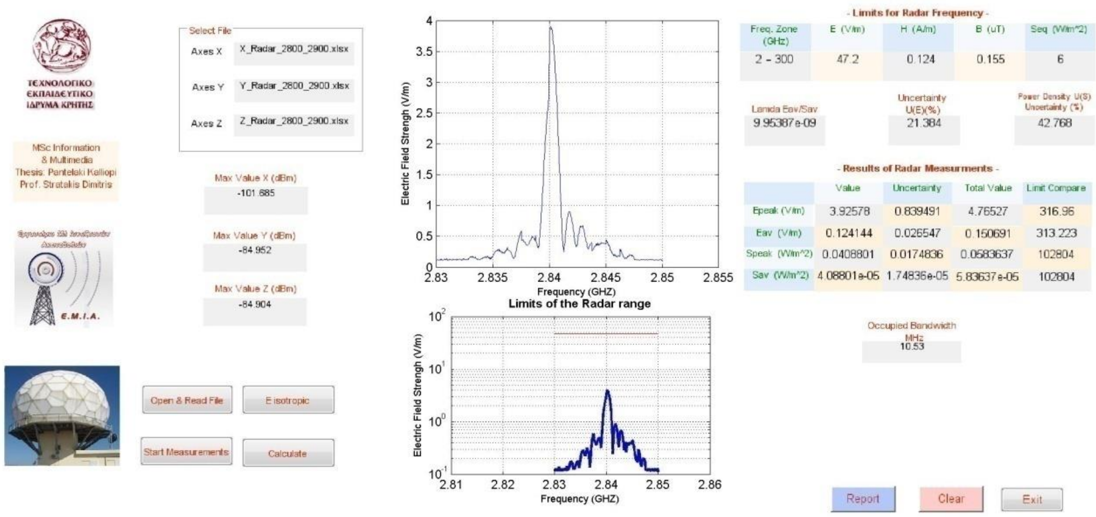

From the above figure of GUI, we come to the conclusion that in the measurement location, PSR Radar radiation emission is within the safety limits.

References

[1] D. Stratakis, A. Miaoudakis, V. Zacharopoulos and T. Xenos, “On the Spatial Averaging of Multiple Narrowband Electromagnetic Field Measurements. Methods and Uncertainty Estimation”, IEEE Trans. Instrum. Meas., Vol.59, no. 6, pp. 1520-1536, June 2010.

[2] UKAS, “M3003, The Expression of Uncertainty and Confidence in Measurement”, 2nd ed., UKAS, Jan. 2007.

[3] D. Stratakis, A. Miaoudakis, T. Xenos and V. Zacharopoulos, “Overall Uncertainty Estimation in Multiple Narrowband in Situ Electromagnetic Field Measurements”, IEEE Trans. Instrum. Meas., Vol. 58, no. 8, pp. 2767-2779, Aug. 2009.

The figures of SA display in the end of measurements.

X polarization

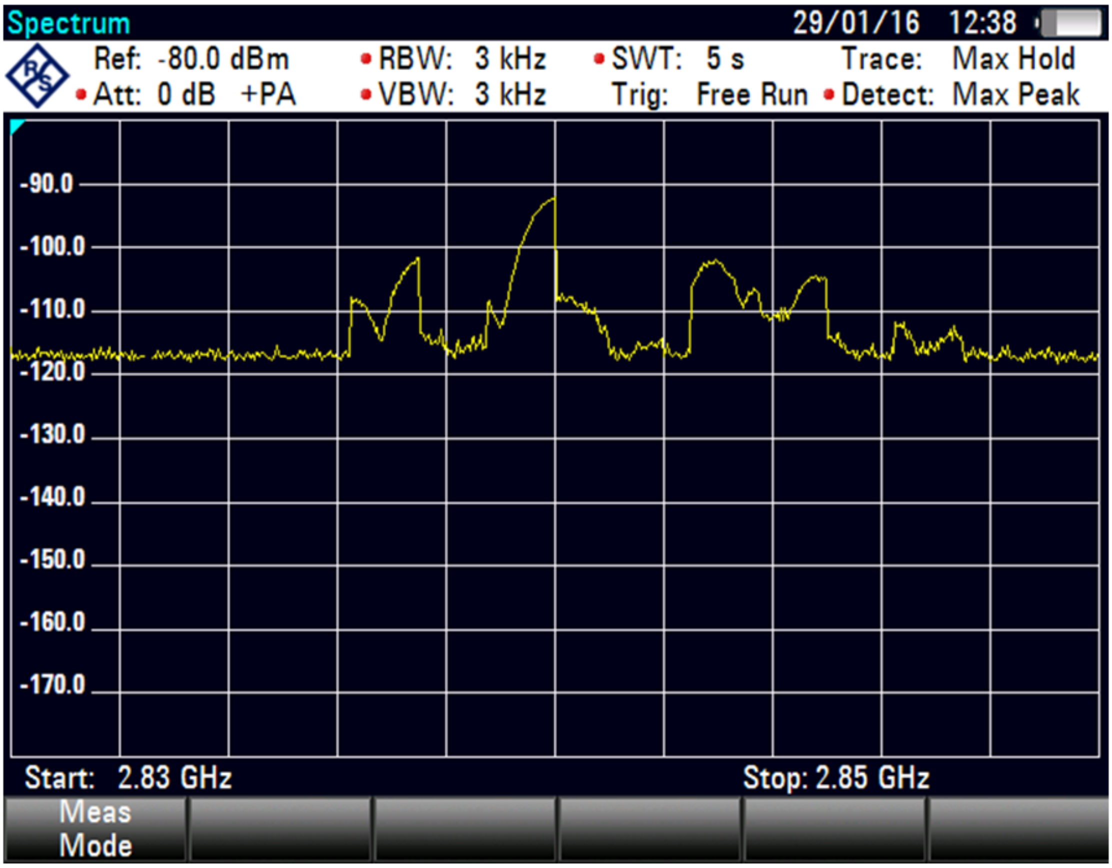

Y polarization

Z polarization

Some pictures during the measurement process

The present report was written according to ELOT 1422-3